5.1 Preformulation study

5.1.1 Development of analytical method

The calibration curve of Hepatitis B surface antigen was linear over the concentration range of 1-25 µg/mL at retention time of 4.8±0.1 min. The equation for the resultant calibration curve was y=2958x+5861 and a linear regression coefficient was found to be 0.9998. Validation of the analytical method for HBsAg in selected condition proved that the designated method was precise and accurate with linear response. The validation parameters are mentioned in Table 5.1. Calibration curve obtained from the HPLC analysis and a representative chromatogram of HBsAg loaded NPs is shown in Figure 5.1.

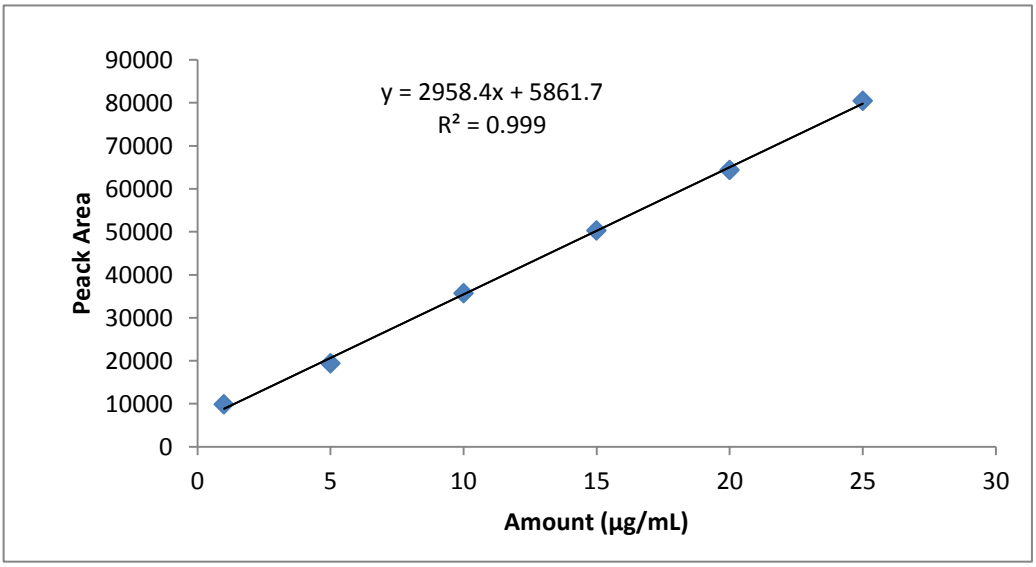

Figure 5.1: Standard calibration curve of Hepatitis B antigen in phosphate buffer saline (pH7.4)

Table 5.1: Analytical method validation parameter

Validation parameter	Results
Standard Regression Equation	y = 2958x + 5861
Regression Coefficients (R^2)	R^2 = 0.9998
λ max.	280 nm
Linearity (µg/mL)	1-25
LOD (ng/ml)	0.979117174
LOQ (ng/ml)	2.967021741

5.2 Formulation of HBsAg loaded polymeric nanoparticles

HBsAg loaded PLGA NPs delivery systems have been developed for improvement of bioavailability, controlled and sustained release of antigen. The antigen carriers like polymeric nanoparticles (NPs) are appropriate for delivering protein, small molecular, peptide and macromolecules by either local or targeted delivery [Moghimi *et al.*, 2001]. Development of nanoparticles is a very tedious procedure, involves various processing variables and design components. Process variables and system components have significant interactions among themselves, which affects the quality of final product. For the development of nanoparticles it is necessary to identify these processing factor and their interactions which gives good formulation attributes and performance characteristics of the product. For this purpose, an experimental technique like Design of Experiment (DOE) was used, which provides rational and scientific way for estimation, identification and influence of critical factors on the quality of product.

The use of factorial design and design expert suggest a possibility of analysing larger number of variables at more levels with very few experimental runs. Even slight

modification in processing and formulation parameters can have significant change in the quality of final product. For example, particle size and entrapment efficiency are most significant parameter of nanoparticles from biological and pharmaceutical point of view. Proper optimization increases the entrapment efficiency and avoid loss of drug during preparation. Therefore, a central composite design model was utilized for the formulation of polymeric nanoparticles. It gives accurate interpretation, minimum number of runs and produce predicted formula for preparation of polymeric nanoparticles.

Total of thirty experimental runs were obtained from four factors, three levels central composite statistical experimental design. The values of responses (dependent variables) are presented in Table 5.2. The quality of the model is assessed by coefficient of determination: R^2, Adj R^2 and Pred R^2, which is shown in Table 5.3. Prepared nanoparticle size range varied from 262.1±4 to 274±9 nm, recommending control of particle size which can be accomplished by varying the levels of four independent variables. Similarly the percentage entrapment efficiency of prepared nanoparticles range varied from 88.5 to 93.1%. After experiment polynomial mathematical equations were found for each response which explained the main effects, interaction effects and quadratic effect of independent variables. Obtained equation for each response can be positive or negative value of independent factor which represents the direct and indirect effect on response [Chopra *et al.,* 2007; Mujtaba *et al.,* 2014].

Table 5.2: Combined effects of the four independent variables on the particle size and entrapment efficiency

Std	Run	Block	Independent Variables				Response	
			Factor 1 A: Polymer	Factor 2 B: PVA	Factor 3 C: Aq/Org. Ratio	Factor 4 D: H. Speed	1:PS (nm)	2:EE (%)
4	1	Block 1	40.00	1.50	1.50	5000.00	273.0	87.9
7	2	Block 1	30.00	1.50	3.30	5000.00	271.9	88.5
9	3	Block 1	30.00	0.50	1.50	15000.00	263.0	90.2
27	4	Block 1	35.00	1.00	2.40	10000.00	266.0	93.1
20	5	Block 1	35.00	2.00	2.40	10000.00	264.3	92.3
16	6	Block 1	40.00	1.50	3.30	15000.00	262.0	92.1
12	7	Block 1	40.00	1.50	1.50	15000.00	264.2	90.5
29	8	Block 1	35.00	1.00	2.40	10000.00	265.0	92.9
3	9	Block 1	30.00	1.50	1.50	5000.00	274.0	87.6
19	10	Block 1	35.00	0.00	2.40	10000.00	266.0	89.0
30	11	Block 1	35.00	1.00	2.40	10000.00	266.6	92.6
18	12	Block 1	45.00	1.00	2.40	10000.00	266.8	89.9
23	13	Block 1	35.00	1.00	2.40	10000.00	266.1	91.2
10	14	Block 1	40.00	0.50	1.50	15000.00	261.9	91.0
2	15	Block 1	40.00	0.50	1.50	5000.00	269.0	87.9
8	16	Block 1	40.00	1.50	3.30	5000.00	268.9	88.9
25	17	Block 1	35.00	1.00	2.40	10000.00	266.6	92.6
5	18	Block 1	30.00	0.50	3.30	5000.00	271.0	91.0
11	19	Block 1	30.00	1.50	1.50	15000.00	263.2	91.0

6	20	Block 1	40.00	0.50	3.30	5000.00	272.1	88.9
24	21	Block 1	35.00	1.00	2.40	10000.00	266.6	92.6
26	22	Block 1	35.00	1.00	2.40	10000.00	266.6	92.6
14	23	Block 1	40.00	0.50	3.30	15000.00	264.1	90.1
15	24	Block 1	30.00	1.50	3.30	15000.00	262.0	90.0
28	25	Block 1	35.00	1.00	2.40	10000.00	266.6	92.6
21	26	Block 1	35.00	1.00	0.60	10000.00	263.0	90.1
1	27	Block 1	30.00	0.50	1.50	5000.00	273.0	89.9
17	28	Block 1	25.00	1.00	2.40	10000.00	266.0	89.6
22	29	Block 1	35.00	1.00	4.20	10000.00	265.3	89.9
13	30	Block 1	30.00	0.50	3.30	15000.00	263.5	90.0

Table 5.3: Estimated model and statistical validation of developed formulation

Response	F value	Df	R^2	Adj R^2	Pred R^2	P value
Particle Size	21.44	14	0.9524	0.9080	0.6741	<0.0001
Entrapment Efficiency	6.68	14	0.8617	0.7327	0.0943	<0.0004

***** R^2: Coefficient of determination (Pure collaboration between measured and predicted value), Adj R^2: Adjusted R^2, Pred R^2: Predicted R^2, DF: Degree of freedom, P value: Significance difference, F value: analysis of variance.

For the particles size and entrapment efficiency two different equations were obtained. The following equation (1) was obtained for the particles size:

$$PS(Y1) = 266.26 - 0.28X1 - 0.075X2 - 0.05X3 - 4.31X4 + 0.025X1X2 + 0.24X1X3 + 0.46X1X4 - 0.84X2X3 - 0.24X2X4 + 0.28X3X4 - 0.091X1^2 - 0.28X2^2 - 0.53X3^2 + 1.93X4^2 \ldots\ldots\ldots\ldots (1)$$

The model was found to depict very low probability value (P>0.0001) which indicated the model was statistically significant. The central composite design model was also evaluate for adjusted determination coefficient (R^2), it is very high (>90%) [Myers and Montgomery, 2002; Dutka *et al*., 2015].

The large value of coefficient suggested that the concentration of PLGA and Aq/Org ratio mainly affected the particle size. The concentrations of PVA and homogenizer speed rate negatively affected the particle size. An increase in the amount of PLGA concentration directly decreased the particle size due to polymer interaction with PVA (Figure 5.2). When amount of Aq/Organic phase ratio was increased larger droplets were broken down by sonication which promoted formation of smaller size droplets. With increase in the percentage of PVA, particle size decreased dramatically, similarly when the homogenizer speed was increased particle size decreased (Figure 5.2 and 5.3). When PVA is present in higher concentration, it aligns themselves at the interface thus inspire stability of the suspension via decreasing the free energy at the interface [Demirel and Kayan, 2012].

Equation for entrapment efficiency: For the maximum drug entrapment, required information about the effects of independent variables on the nanoparticles properties were obtained. All the data describing the relationship between four independent variables and percentage of entrapment efficiency are shown on Table 5.2. The percentage of entrapment efficiency in the PLGA nanoparticles varied.

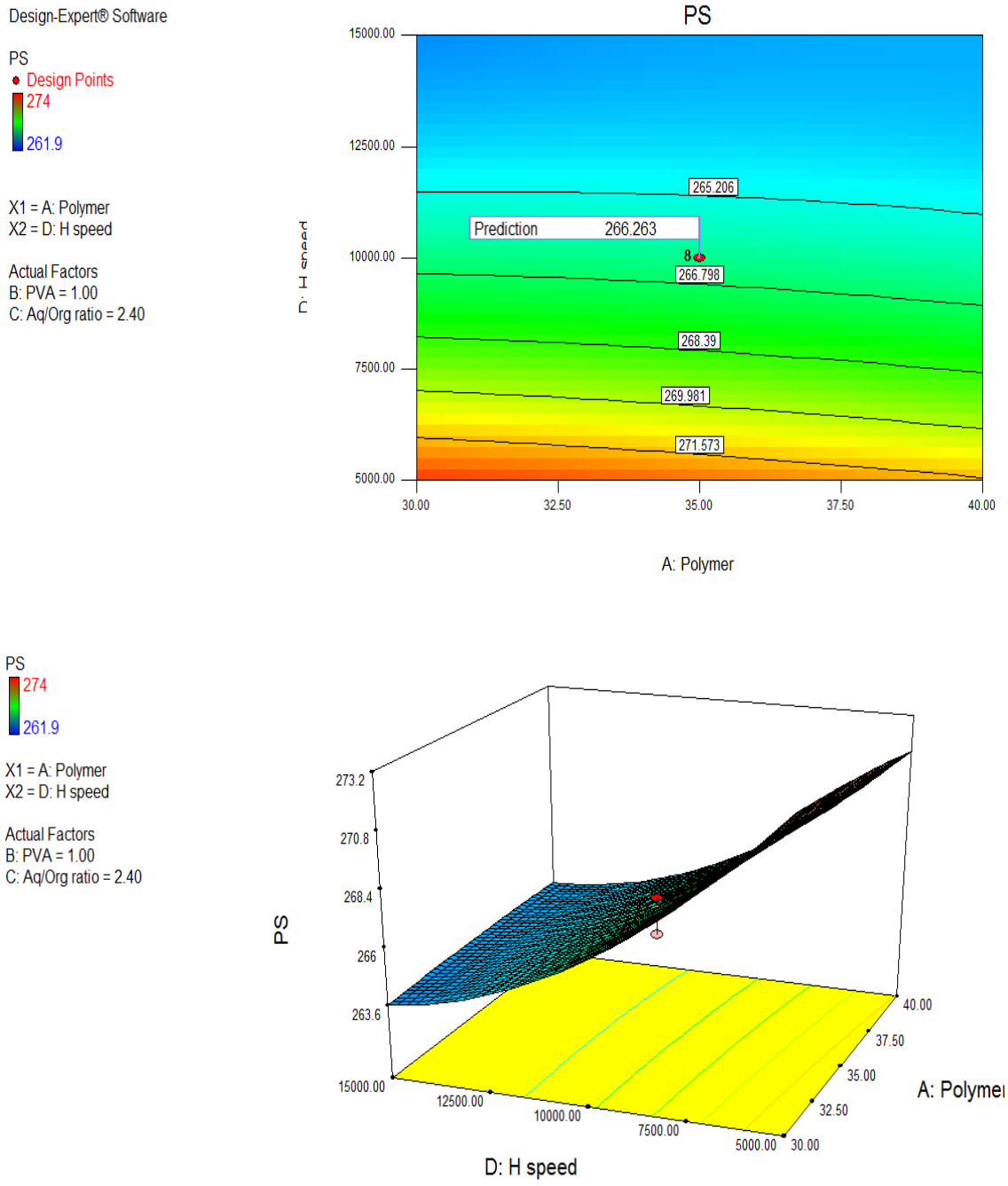

Figure 5.2: Two and three dimensional graphical illustrations demonstrating the interaction between the polymer concentration and homogenization speed on particle size

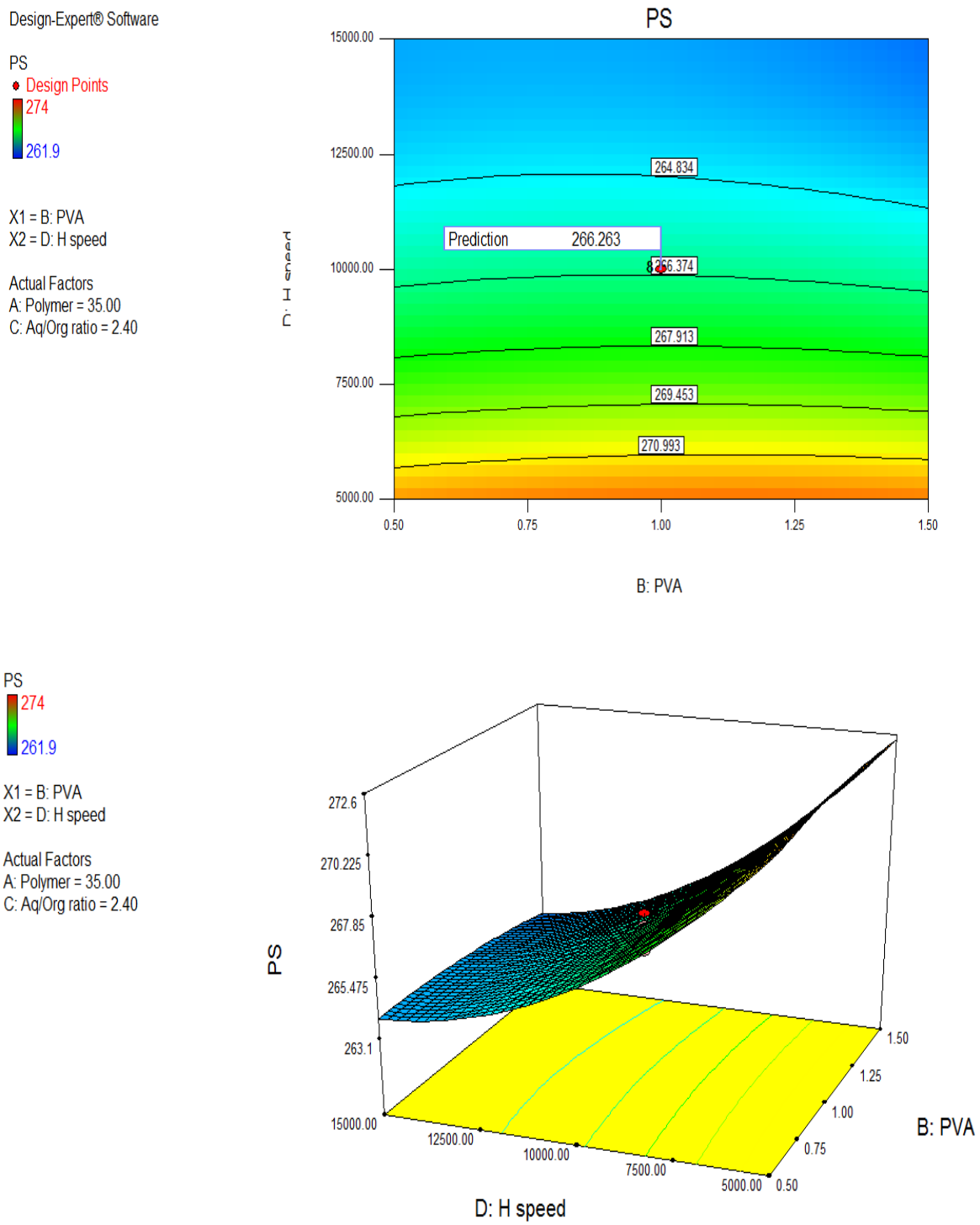

Figure 5.3: Two and three dimensional graphical illustrations demonstrating the interaction between the percentage of PVA and homogenization speed on particle size

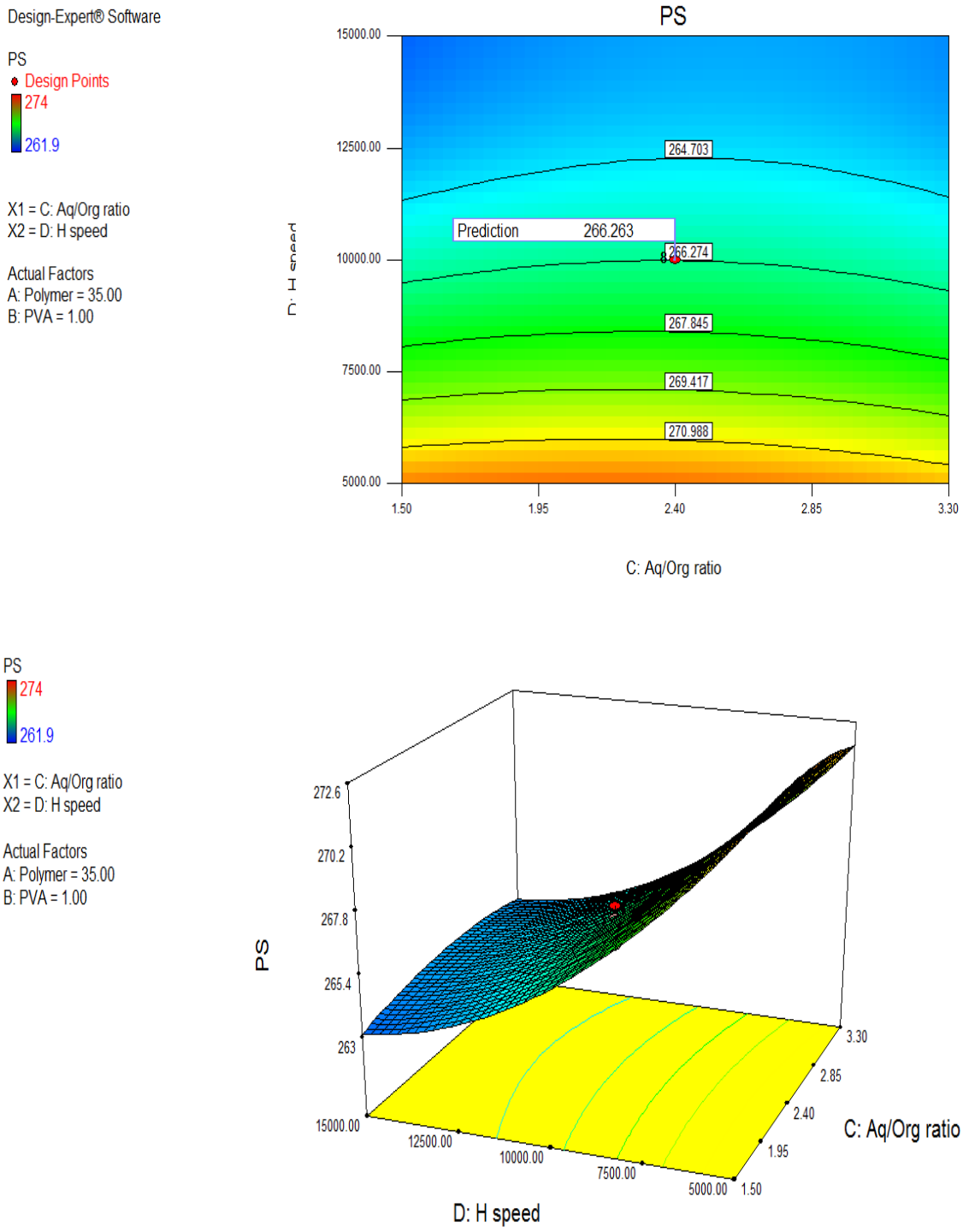

Figure 5.4: Two and three dimensional graphical illustrations demonstrating the interaction between the Aq/Org ratio and homogenization speed on particle size

The highest entrapment was obtained when factors X1, X2, X3 and X4 were in their medium level (0). A second-order polynomial model to fit these data is shown below equation (2):

$$EE=92.53-0.013X1+0.17X2+0.13X3+0.89X4+0.34X1X2+0.12X1X3+0.37X1X4 +0.094X2X3+0.44X2X4-0.28X3X4-0.69X1^2-0.47X2^2-0.63X3^2-1.01X4^2 \ldots\ldots (2)$$

The formulation design model suggested the good predictability and variables shows good response for all (% error <5%) and included value of F-statistics results showed a low probability value which revealed that the model was statistically significant. The adjusted R^2 was very high, indicating that the model fitted the data very well. The positive signs for the coefficient of X1, X2, X3 and X4 in equation 2 suggested that, the entrapment efficiency of loaded drug increased with the increase of X1, X2, X3 or X4. The PLGA concentration (X1) predominantly influences the drug encapsulation over the other variables. Also the PVA concentration (X2) had a strong quadratic influence in formulation development and Aq/Org phase ratio shows minor influence (Figure 5.5 and 5.6), whereas the homogenizer speed rate showed a major effect on particle size as well as entrapment efficiency [Galindo-Rodriguez *et al.,* 2004].

An increase in the PLGA concentration in formulation, increases the viscosity of the organic phase that separates the two aqueous layers, this reduce the drug diffusion into the external aqueous phase. When the PLGA concentration increased it means the large particles size and larger particles have more volume for incorporation of more drug into the particle, thereby increasing drug entrapment efficiency. An increase in PVA concentration also increased the drug encapsulation. An increase in the PVA concentration also increased the viscosity of the external aqueous phase [Illum *et al.,* 1986; Kollipara *et al.,* 2010]. However, high homogenization speed resulted in

decreased drug adsorption to the particle surface due to the rapture of the particle. Thus, to prepare nanoparticles a definite speed homogenization is required.

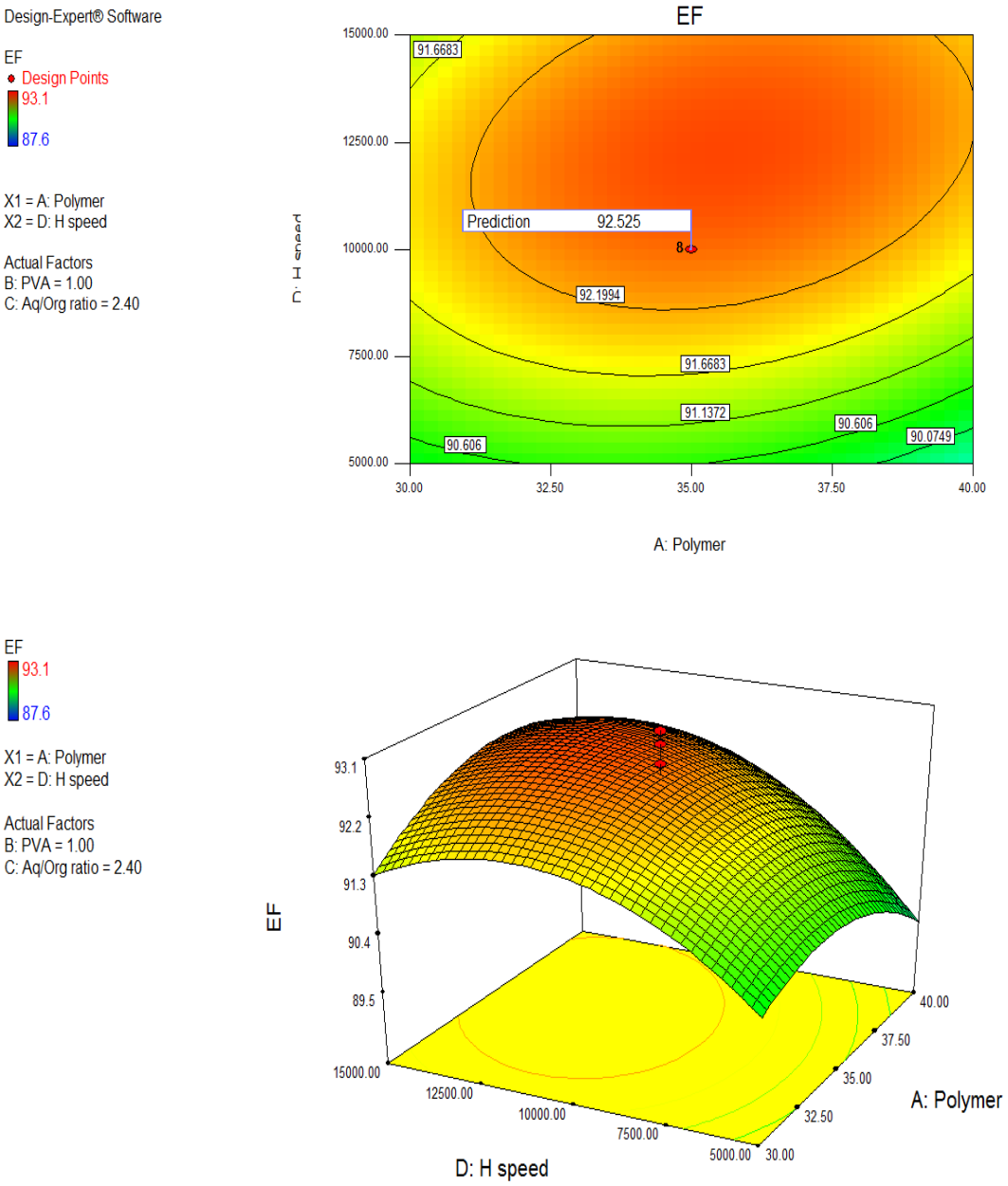

Figure 5.5: Two and three dimensional graphical illustrations demonstrating the interaction between the homogenizer speed and polymer concentration on entrapment efficiency

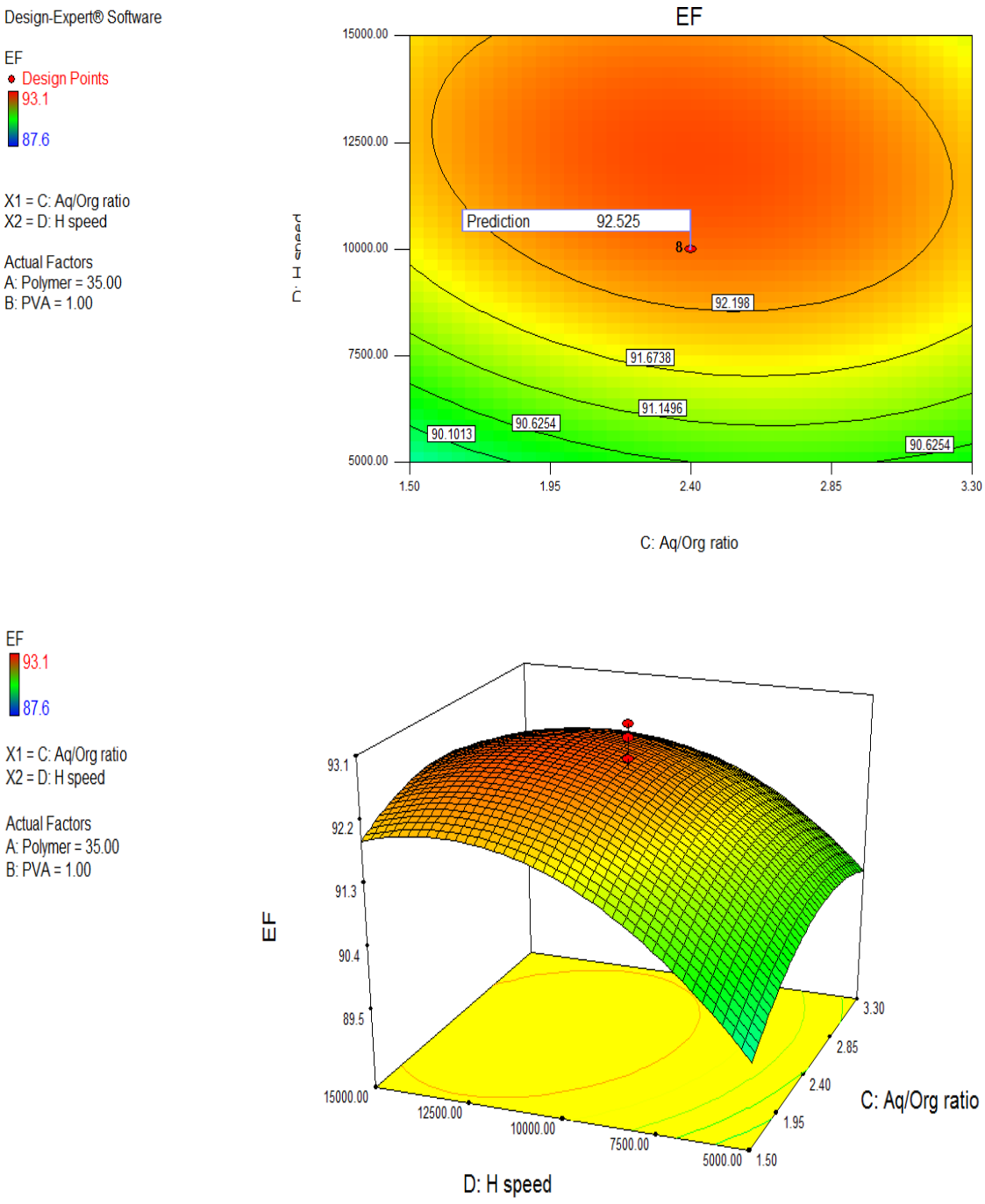

Figure 5.6: Two and three dimensional graphical illustrations demonstrating the interaction between homogenizer speed and Aq/Org ratio on entrapment efficiency

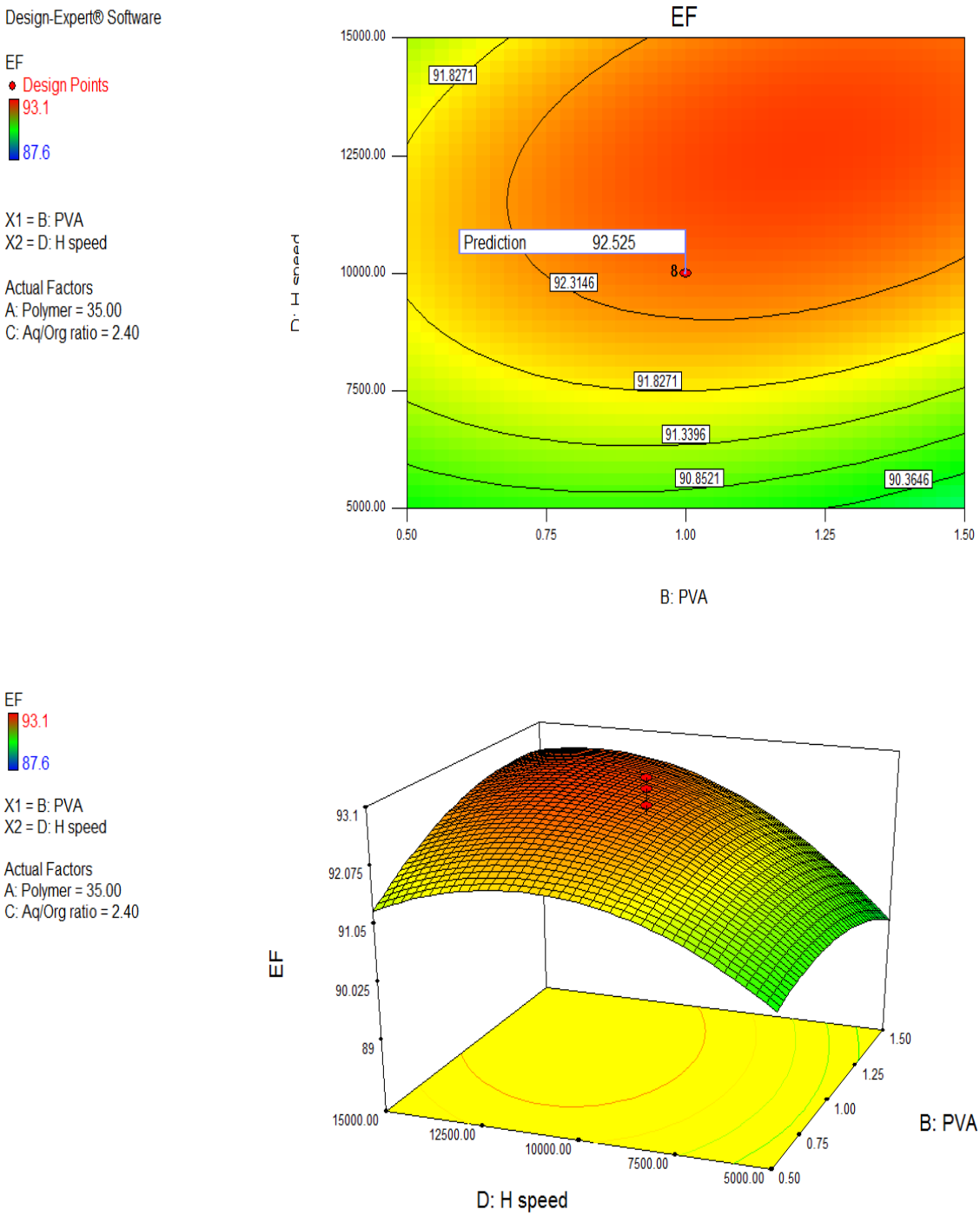

Figure 5.7: Two and three dimensional graphical illustrations demonstrating the interaction between homogenizer speed and percentage of PVA on entrapment efficiency

- **Optimization validation and experimental prediction**

The final optimized batch was performed by numerical method through maximum desirability factor. The predicted values of particles size and entrapment efficiency were found to be 266.203 nm and 92.525%, respectively at the polymer concentration (35 mg), PVA (1%), Aq/Org ratio (2.4) and homogenizer speed (9950.33 rpm) as shown in Figure 5.8. Therefore, new experimental batch of antigen with predicted levels of independent variables was prepared to confirm the validity of optimization. The desirability for each formulation were observed but the final optimized formulation batch which having the overall highest desirability value was attained by 35 mg PLGA, 1% w/v PVA, Aq/Org phase ratio 2.4 and 10000 rpm of homogenizing speed. The resulted nanoparticles showed the 92.52% antigen entrapment efficiency and 266.6 nm optimized particles size (Table 5.4).

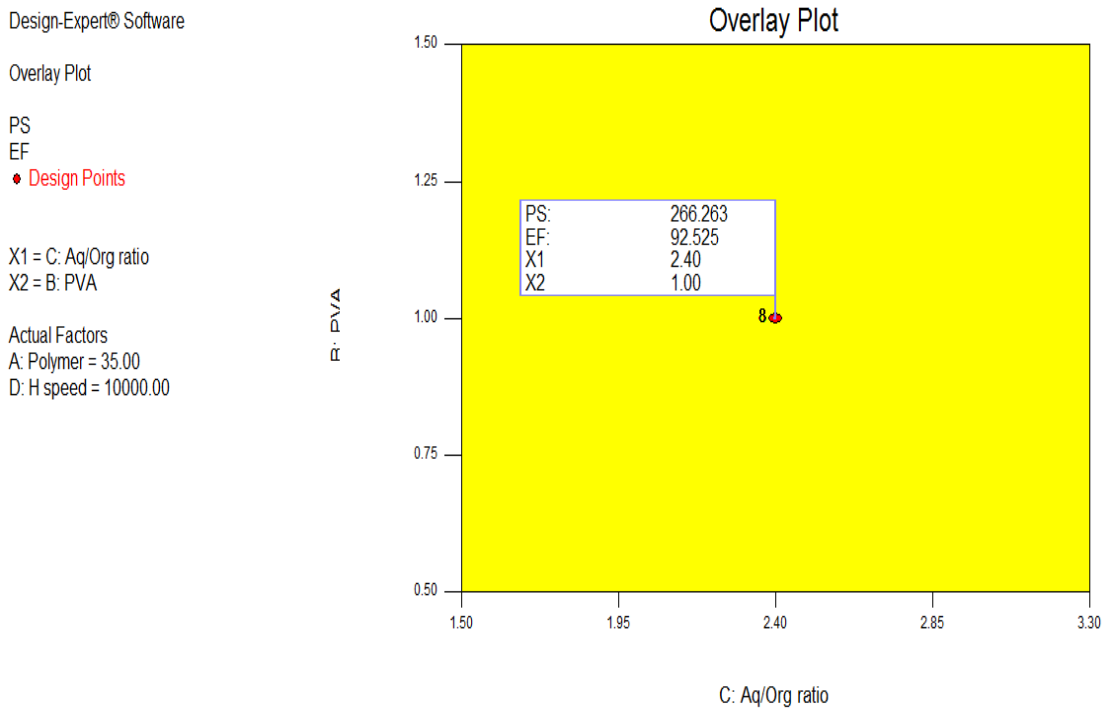

Figure 5.8: Desirability graph of predicted optimized batch

The results indicated the reliability of the model because the predicted value is in good agreement with observed experimental value. The nanoparticles size range and entrapment efficiency have been suitable for good internalization so that this optimized HBsAg loaded nanoparticles batch was selected for the further *in-vitro* characterization and *in- vivo* study.

Table 5.4: Optimal predicted and experimental batch with dependent and independent process variables

Batch	Composition and process variables				Response	
	Polymer (mg)	PVA (%)	Aq/Org ratio	H. Speed (rpm)	PS (nm)	EF (%)
Predicted	35.00	1.0	2.40	9950.33	266.3	92.5
Experimental	35.00	1.0	2.40	10000.00	266.2	92.5

Freeze drying of nanoparticles: The long term stability of nanoparticles can be improved by formulating the systems as completely freeze-dried products (Figure 5.9).

Figure 5.9: Freeze drying of HBsAg loaded nanoparticles preparation

5.3 *In-vitro* characterization of polymeric HBsAg loaded nanoparticles

- **Particle size, polydispersity index and zeta potential**

Nanoparticles exhibited good polydispersity and were in nanometric size range as evaluated by Beckman Coulter particle size analyzer. The average particle size of optimized batch was found to be 266±0.03nm. The particles size distribution curve is shown in Figure 5.10.

Zeta potential is one of the essential parameters to evaluate stability of any colloidal system. Diffraction light scattering was used for zeta potential as well as polydespesity index measurements. The zeta potential of optimized antigen loaded PLGA nanoparticles was found to be -41.58±0.5 mV (Figure 5.11). The negative value of zeta potential is due to nonionic nature of surfactant. However, it foremost depends on the chemical nature and interaction between polymer, surfactant and drug concentration.

- **Entrapment efficiency**

The entrapment efficiency of developed formulation was evaluated by RP-HPLC method and EF of optimized batch was found to be 92±5%.

Particle size and entrapment efficiency greatly influenced the homogenizer speed. A significant increase in homogenizer speed decreases the particle size. Homogenizer speed is inversely proposal to the particle size, whereas entrapment efficiency was directly proportional to homogenizer speed and mostly unaffected.

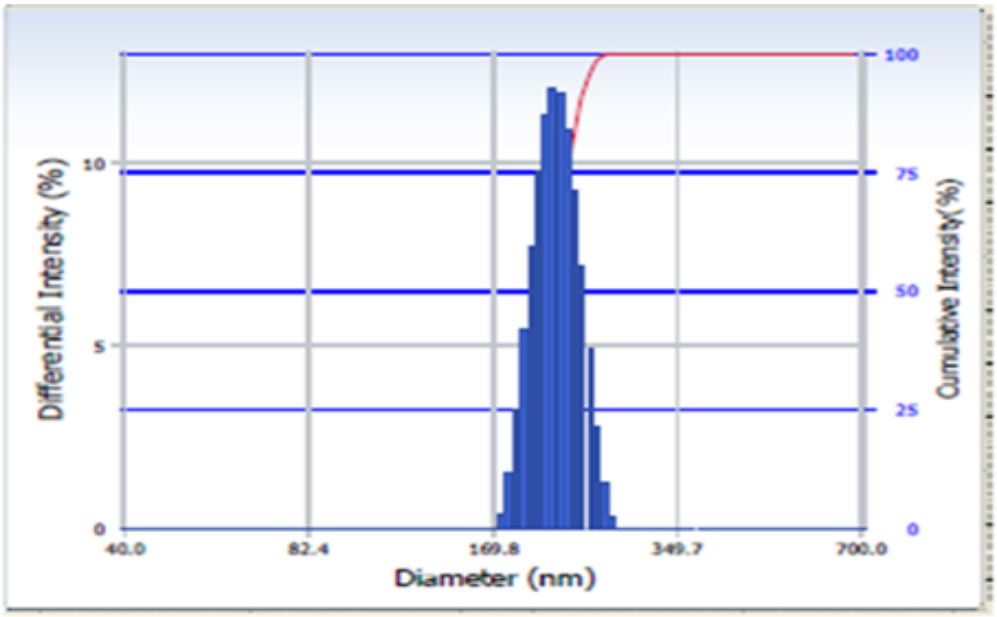

Figure 5.10: Particle size destruction curve of HBsAg loaded nanoparticles

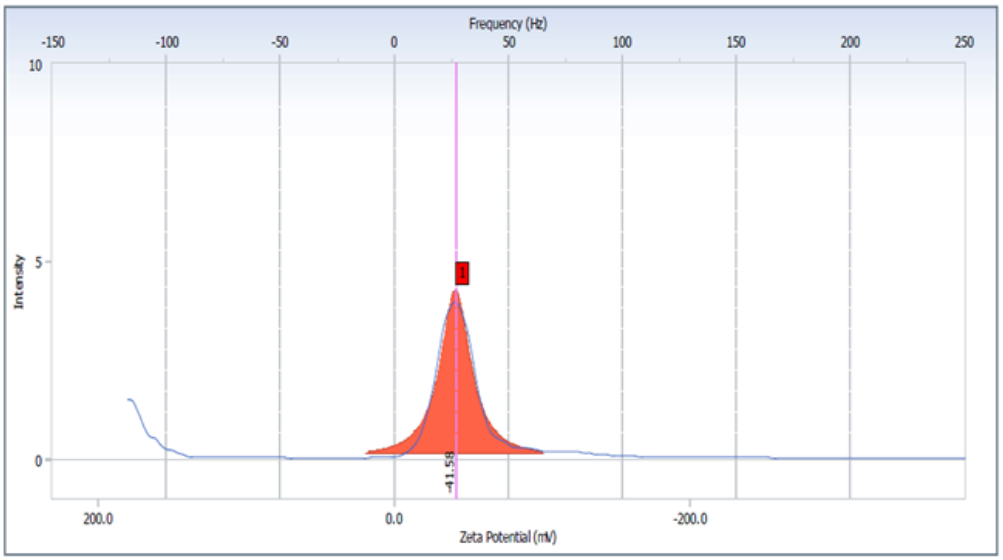

Figure 5.11: Zeta potential analysis of HBsAg loaded nanoparticles

5.4 Surface characterization

The morphology of antigen loaded PLGA nanoparticles was analysed and most of the nanoparticles were uniform and fairly spherical in shape. The particle surface also showed a characteristic smoothness (SEM image, Figure 5.12). In transmission electron microscopy (TEM) observations, polymer layer was found adhered to the particle. No breakage or tear was noticed (Figure 5.13).

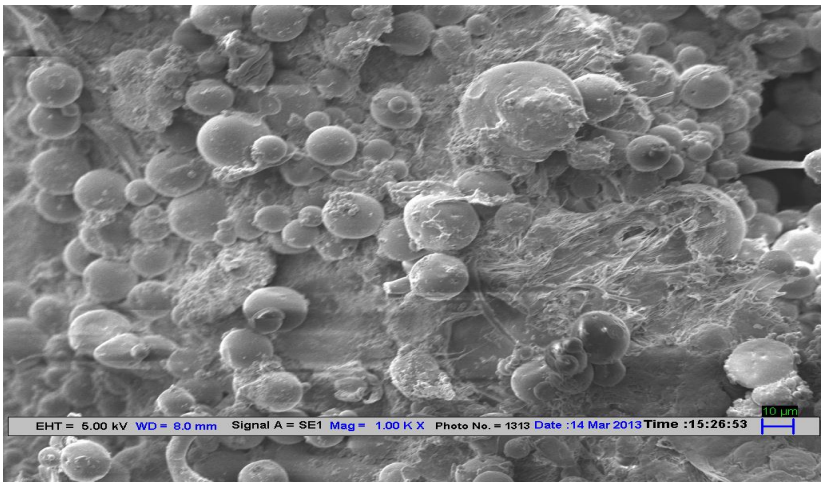

Figure 5.12: SEM photographs of antigen loaded nanoparticles

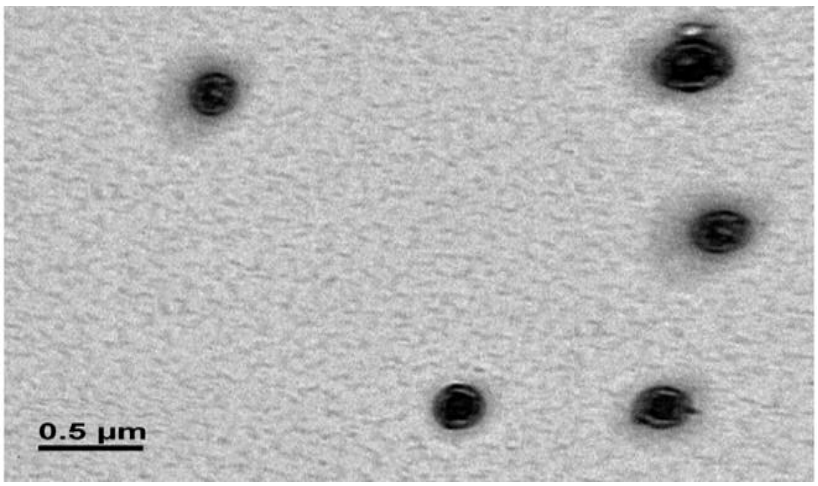

Figure 5.13: TEM photographs of antigen loaded nanoparticles

AFM image of HBsAg loaded NPs has showed good agreement and size was determined by dynamic light scattering and transmission electron microscopy methods. The particles shape parameters were compared by determining the average roughness, kurtosis and skewness of prepared formulation (Table 5.5). Kurtosis indicates whether the data is heavy-tailed or light-tailed relative to a normal distribution. The found kurtosis value is high tends to have heavy tails, or outliers. Data sets with low kurtosis tend to have light tails, or lack of outliers.

Skewness is a measurement of symmetry in distribution of NPs in media (more precisely, the lack of symmetry). If skewness is positive, the data is positively skewed or skewed right, meaning that the right tail of the distribution is longer than the left. If skewness is negative, the data is negatively skewed or skewed left, meaning that the left tail is longer. Zero value of skewness indicates perfect symmetrical data. Two dimensional and corresponding three dimensional views of NPs are shown in Figure 5.14 and 5.15. The average height of loaded nanoparticles was found to be 216- 308 nm. The average height of loaded nanoparticles through AFM was not significantly different than particle size calculated through DLS ($P<0.05$). The photographs revealed the actual morphology of nanoparticles. Majority of the particles were spherical in shape. Apart from spherical shape, few disc like shapes were also found in these photographs.

Table 5.5: Various surface characters of nanoparticles

S.No.	Surface Character	Measurement
1	Average roughness	0.106 nm
2	Skewness	0.00536
3	Kurtosis	3.019

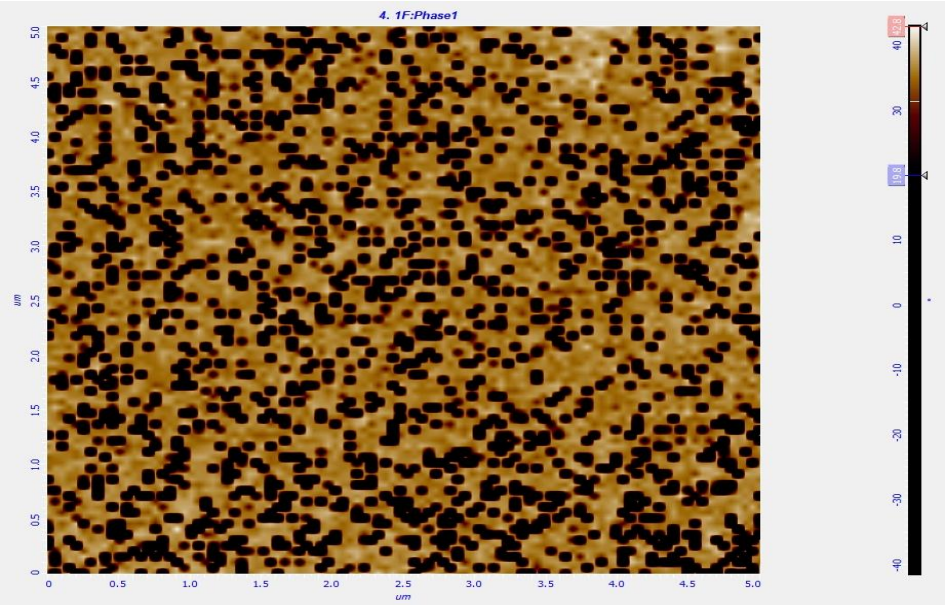

Figure 5.14: 2D, AFM photographs of antigen loaded nanoparticles

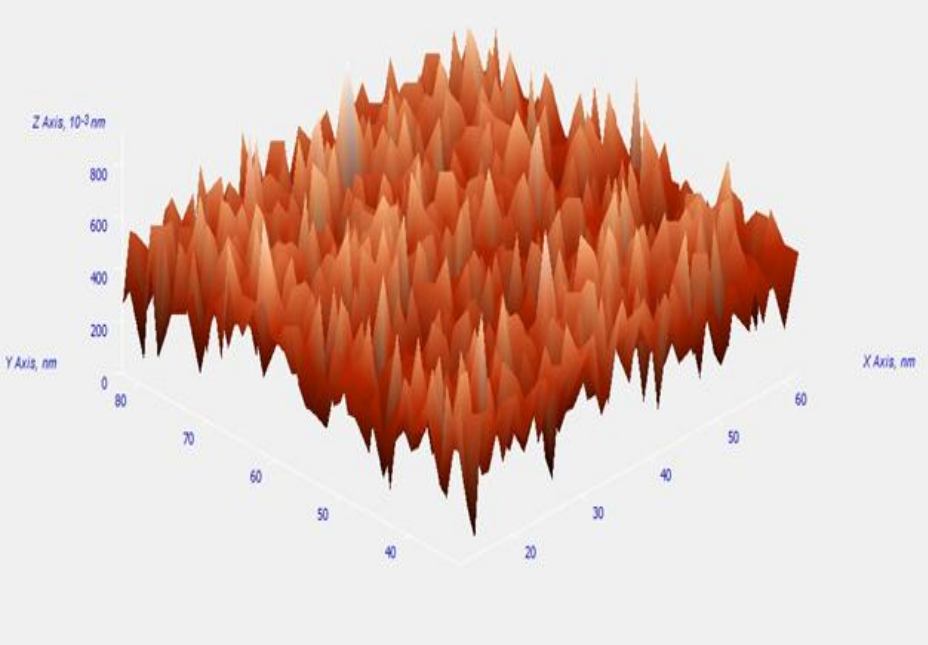

Figure 5.15: 3D, AFM photographs of antigen loaded nanoparticles

5.5 *In-vitro* release of HBsAg from nanoparticles

The biodegradable polymeric systems have been developed as good contestants since they provide adjuvancity with prolonged sustained release characteristics. When an antigen is associated with this particulate polymeric PLGA carriers system, it generates a stronger immune response compared to soluble antigen [Raghuvanshi *et al.*, 2002]. The antigen release kinetics provides critical information about behaviour of dosage form that can be used to assess product safety and efficacy. Actually, *in-vitro* release testing is commonly used to predict *in-vivo* behaviour. *In-vitro* release studies are conducted to measure the rate and extent of compound transported across the blood capillaries. The rate of release depends on presence of polymer in the formulation. The mean cumulative release profile of optimized batch of Hepatitis B surface antigen from nanoparticles is represented in Figure 5.16. The percentage cumulative release profile of HBsAg loaded nanoparticles was 90–92% in 36 days.

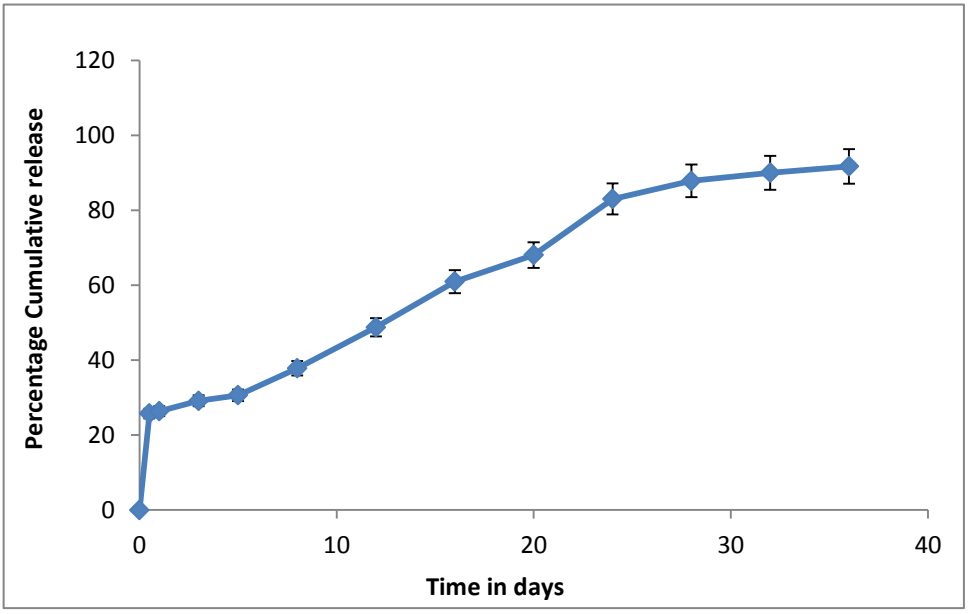

Figure 5.16: *In-vitro* release of antigen loaded nanoparticles in PBS (pH 7.4)

The nanoparticles exhibited sustained drug release. The drug release mechanism was determined by plotting the release data to various kinetic models and comparing with different correlation coefficient values presented in Table 5.6. Zero order (R^2 = 0.974) was found most satisfactory to describe the release kinetics. Therefore, the drug release mechanism was assumed to be controlled. In Higuchi and Korsmeyer–Peppas model, the release exponent was found to be 0.947 and 0.862 respectively, indicating the release of antigen by diffusion mechanism (Figure 5.17), because of degradation of the matrix, although several other release mechanisms could be involved, including surface and bulk erosion, diffusion, disintegration and desorption. The exponent n value is below 0.5 which means the drug is release through fickian diffusion. The NPs formulation showed an initial burst release, leading to rapid release of adsorbed antigen on to the surface of the nanoparticles.

Table 5.6: Correlation coefficient value of HBsAg loaded nanoparticles

Release kinetic model	**Zero order**	**First Order**	**Higuchi model**	**Korsmeyer-Peppas model**
Correlation coefficient value (R^2)	0.974	0.967	0.947	0.862

The ideal delivery of drugs would follow zero order kinetics, wherein blood levels of antigens would remain constant throughout the delivery period *i.e.* constant antigen release from a delivery device such as polymeric matrix system. Prepared HBsAg loaded nanoparticles showed zero order release kinetic. It is proved that the physicochemical properties of the drug as well as polymer and drug to polymer ratio

governs the release of drug from the formulation and release kinetics accordingly [Singhvi and Singh, 2011].

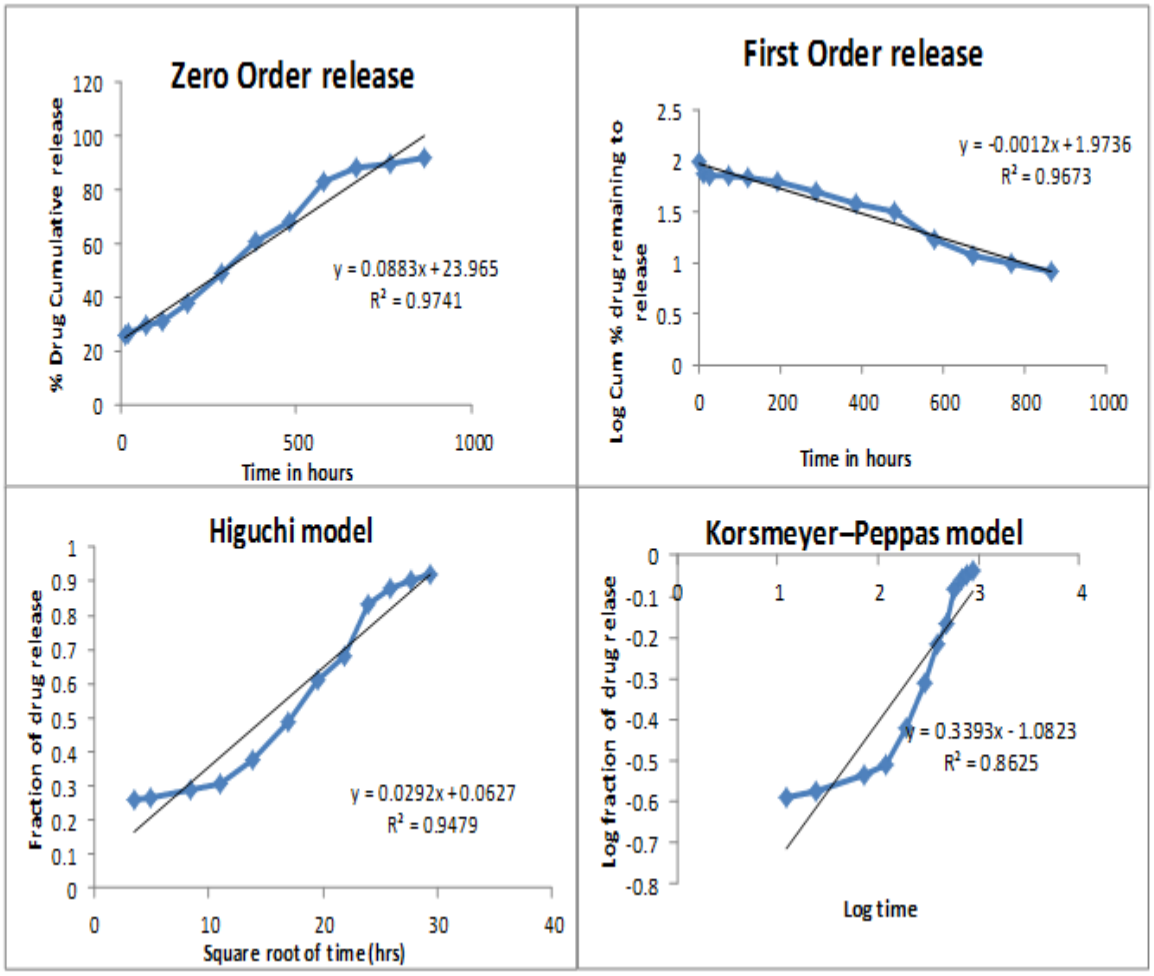

Figure 5.17: *In-vitro* release of Antigen loaded nanoparticles in PBS at pH 7.4 using different kinetic models: Zero order, First order, Higuchi model and Korsmeyer–Peppas model

5.6 Structural integrity of HBsAg loaded nanoparticles

The structural integrity of the nano encapsulated HBsAg was confirmed by SDS–PAGE gel electrophoresis. Electrophoresis analysis followed by silver staining exposed identical and visualized bands for the native and entrapped antigen (Figure 5.18). The encapsulation of antigen in PLGA nanoparticles involves the use of organic solvents and harsh shearing conditions and this can cause alteration of the susceptible moieties. This was confirmed that there was no aggregation and fragmentations of the antigen during antigen encapsulation and its release. The band of HBsAg loaded nanoparticles was found similar to the band of control (pure antigen). Also a similar band was observed with marketed alum adsorbed antigen.

The results indicate that there was no change in the structure of antigen and no interaction between the polymer and antigen. The HBsAg only gets adsorbed or encapsulated in polymeric shell. The antigen was easily encapsulated and adsorbed on polymer surface and maintained its integrity. The polymer was found neither ruptured nor dissolved throughout experiments. Most of the antigens gets adsorbed or encapsulated in polymeric shell. The antigen is hydrophilic in nature and has water soluble globular proteins that maintain their native conformation [Lodish *et al.*, 2002].

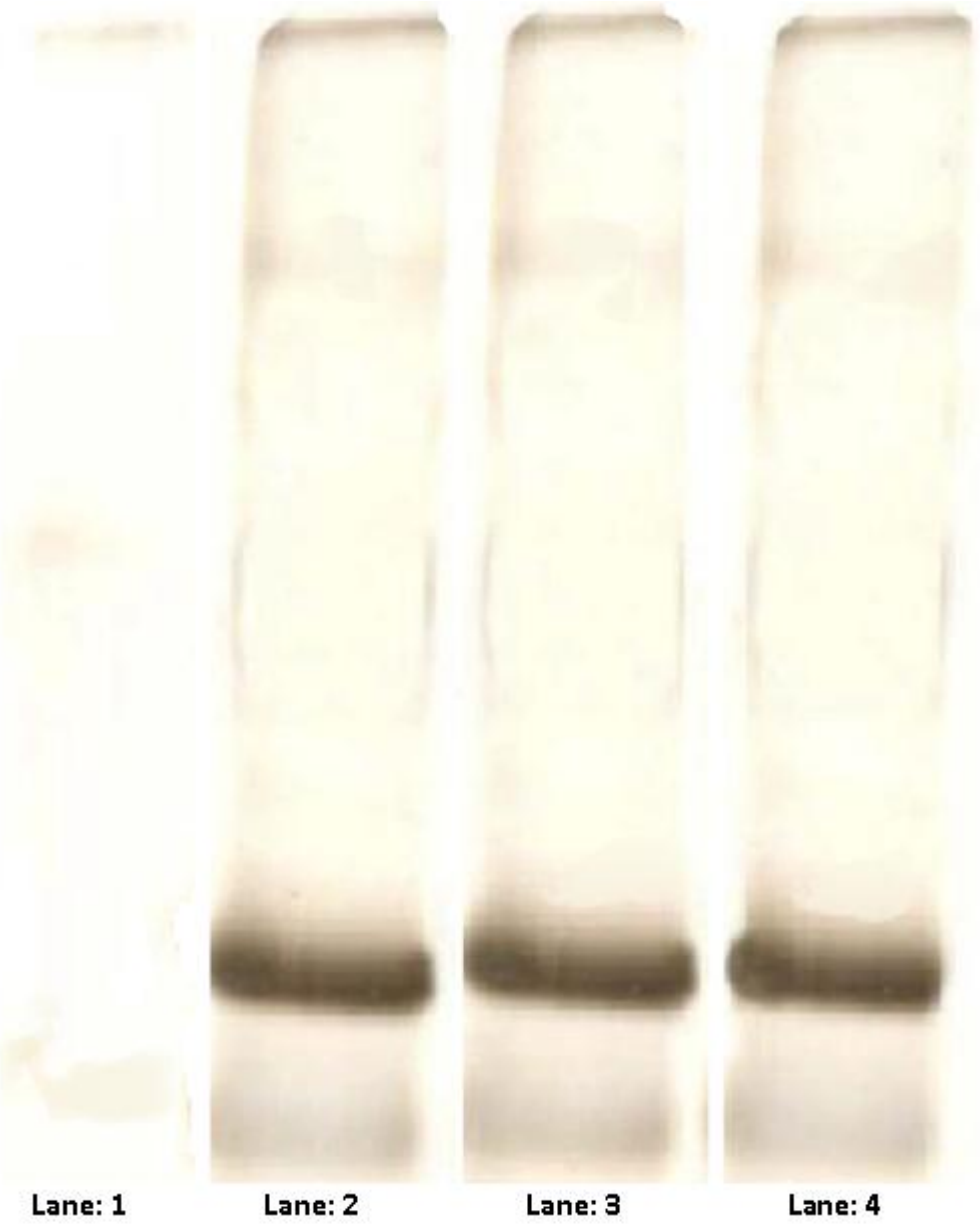

Figure 5.18: SDS–PAGE electrophoresis. Lane 1: distilled water, lane 2: plain HBsAg antigen (control), Lane 3: Alum HBsAg, Lane 4: HBsAg-NPs

5.7 *In-vitro* cellular uptake study of nanoparticles

Labelled NPs loaded with HBsAg was studied after 24 hr incubation by spectral bio-imaging system that delineates the intracellular delivery of NPs to human macrophages. The results clearly suggest better internalization efficacy of HBsAg loaded nanoparticles in short duration. Macrophage is small blue disk in shape, under the fluorescence microscope against black background. Inside the macrophage, various small white dots were observed (Figure 5.19 (a) and (b)). These white dots are nanoparticles which were uptaken by the macrophage cell. In normal macrophages dots were not observed, but nanoparticles treated macrophage white dots of nanoparticles were noticed. Actually, macrophages and phagocytic cells of innate immune system are located in various tissues and derived from bone marrow precursor cells that are develop into monocytes. It is associated with expression of specific membrane receptors for cytokines. These cytokines are secreted by interferon gamma (IFN-γ) and helper T cells, which are the most strong macrophage activators. Macrophages initiate the immune response against microorganisms; they express major histocompatibility complex (MHC) class II molecules on their membranes. When macrophages engulf microbes recognised by T lymphocytes, various cytokines gets released and activate B cells and finally secrete the specific antibodies [Duque and Descoteaux, 2014].

Similarly, internalization of polymeric nanoparticles was observed, when incubated in MRC-5 cell lines (Figure 5.19 (c) and (d)). MRC-5 cell is a normal lung fibroblast cell line, elicited by the components of innate and adaptive immunity. MRC-5 cells look like a pink disk shaped, under the fluorescence microscope against black background. Inside the cells various small white dots were observed. This indicates internalization of nanoparticles in short duration. The internalization mechanism involves direct

translocation or formation of pore transient or endocytosis process. Several bioactive molecules must reach the cytosol in order to mediate their biological effect. Protein and peptides are best candidates for cytoplasmic delivery in terms of total uptake process [Yang and Hinner, 2015].

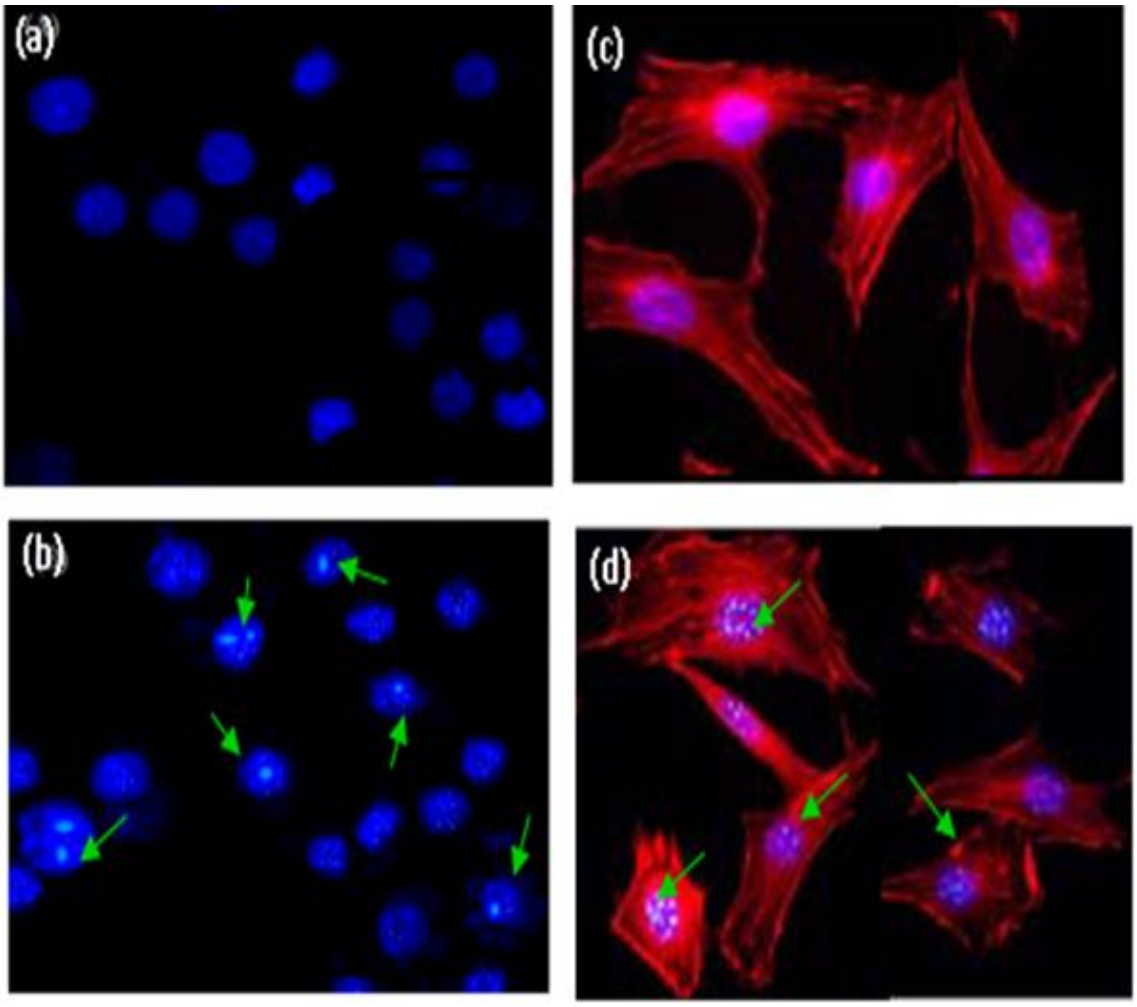

Figure 5.19: Bio-imaging analyses of (a) normal macrophages (b) macrophages incubated with nanoparticles (c) normal MRC-5 cells (d) MRC-5 cells incubated with nanoparticles. The arrows indicated nanoparticles uptake by nucleus of the macrophages and MRC-5 cell line

The quantification of nanoparticles uptake is essentially important to evaluate the fate of tuned nanoparticle in order to increase drug delivery with nanovectors, and also to develop NPs safe by design [Feliu *et al.,* 2016; Brayden *et al.,* 2015; Frohlich, 2012]. The polymeric HBsAg NPs have sizes similar to those of biological molecules and assemblies such as proteins or viruses. They are able to invade the cells and uptake the cellular endocytosis machinery [Bakand and Hayes, 2016; Jha *et al.,* 2017].

The efficiency of nanoparticle carrier molecules for intracellular delivery mainly depends on their interactions with the cell membrane and uptake mechanism. Mainly, nanoparticles interact with extracellular biomolecules that are present in the body fluids, including sugars, proteins and lipids, prior to their encounter with plasma membrane of the cells [Treuel *et al.,* 2014]. Therefore, a FACS analysis was performed to measure nanoparticles uptake. The cell associated fluorescence was evaluated to assess intracellular trafficking of the carriers. In this, cells were incubated with various FITC conjugated NPs and analysed at different time intervals (Table 5.7). A steady increase in the percentage (%) uptake was recorded and maximum cell associated fluorescence for different systems were tested. After 24 h, % uptake in macrophage has followed the order: HBsAg loaded NPs> Alum HBsAg> plain HBsAg> blank NPs (Figure 5.20). The HBsAg loaded nanoparticles showed maximum uptake. Most of the nanoparticles were found to be internalized into cells by endocytic mechanisms. The polymeric nanoparticles were also uptaken by passive penetration through plasma membrane [Khalil *et al.,* 2006; Rothen-Rutishauser *et al.,* 2006; Wang *et al.,* 2012]. Penetration and the ability of nanoparticles to adhere into cell membranes depends upon their size, physical properties, surface composition and charge. However, the prepared polymeric nanoparticles having nano meter size showed greater uptake by the cell [Verma *et al.,* 2008].

Table 5.7: Percentage uptake of Blank NPs, Plain HBsAg and HBsAg loaded NPs after 24 hr.

Time (hr.)	Blank NPs (%)	Plain HBsAg (%)	Alum HBsAg (%)	HBsAg NPs (%)
0	2.5	3.5	4.7	4.5
0.5	6.5	8.5	9.7	9.5
1.0	12	15	21.6	21.5
2.0	20	28	40.1	40
4.0	28	36	50	51
8.0	35	48	62	64
16.0	42	53	67.5	70
24.0	46	56	81	86

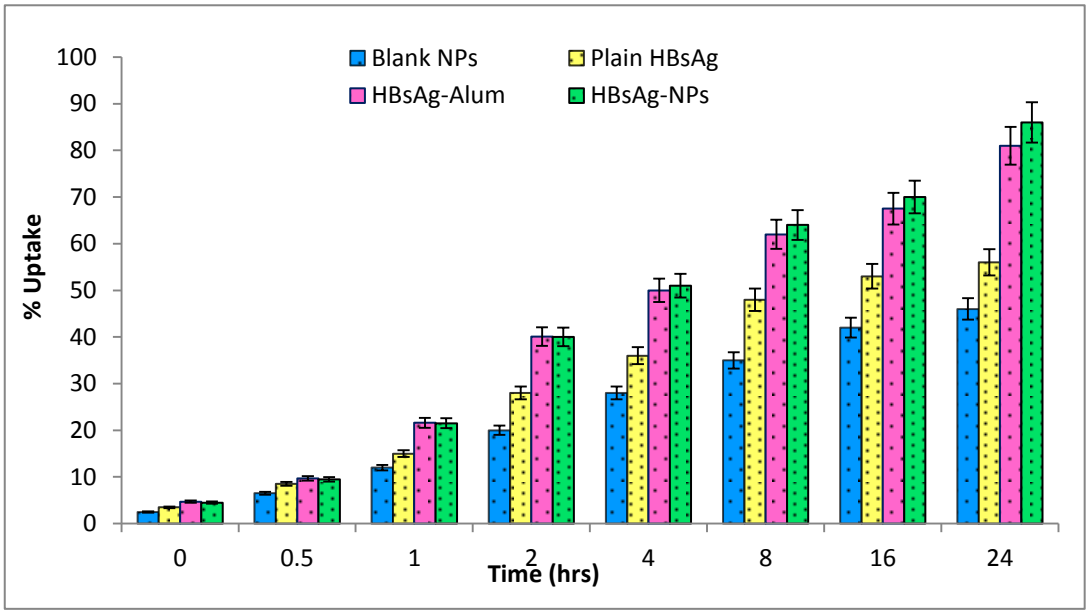

Figure 5.20: Percentage uptake of blank NPs, Plain HBsAg, Alum HBsAg, HBsAg-NPs in 24 hr.

5.8 Haemocompatibility studies

5.8.1 Evaluation of haemolysis

Evaluation of haemolysis is one of the most common study to test the interaction of nanoparticle with blood components, which is necessary to prove the safety of NPs. When nanoparticles are intended for biomedical application, they must be subject to biocompatibility testing before regulatory approval for administration to patients. For these purpose, nanoparticles formulations are prepared for I.M. administration. Comparative haemolysis results of placebo-NPs, plain HBsAg, alum HBsAg and HBsAg NPs at 10, 20 and 30 ng/mL equivalent concentrations are shown in Figure 5.21 [(a), (b) and (c)], respectively.

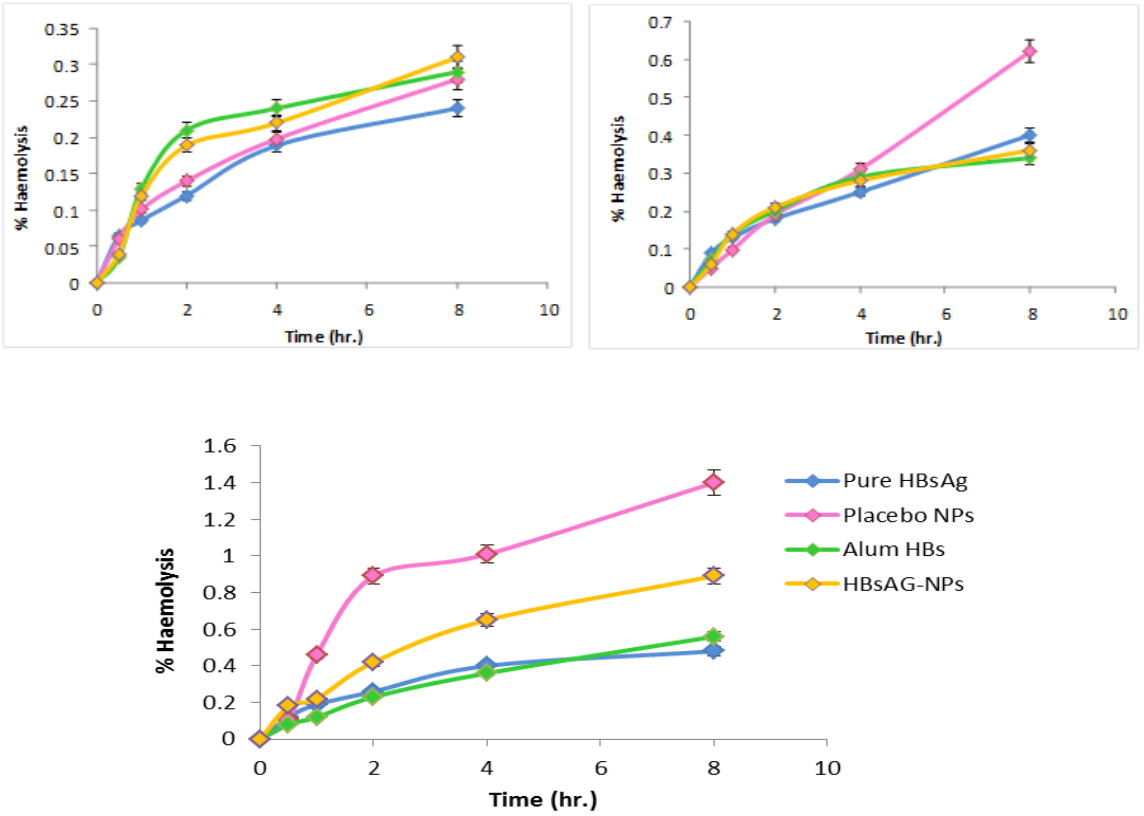

Figure 5.20: Percentage of haemolysis at different time intervals in whole blood samples after incubating with (a) 10 ng/mL (b) 20 ng/mL and (c) 30 ng/mL of Pure HBsAg, Placebo-NPs, Alum HBsAg and HBsAg NPs

HBsAg NPs showed haemolysis value of ≤1% in all equivalent concentrations throughout the study period (8 h). Similarly alum HBsAg showed almost haemolysis equivalent to HBsAg NPs. Haemolysis of placebo-NPs at 10 ng/L equivalent volume was found to be statistically similar to HBsAg NPs ($p>0.05$). Similarly, at 20 ng/mL equivalent volume, placebo-NPs showed significantly similar haemolysis value at 8 hr than that of HBsAg NPs ($p>0.05$). At 30 ng/mL equivalent volume, haemolysis value of Placebo-NPs was found to be significantly higher at 4 and 8 hrs in comparison to HBsAg NPs. Though all components of Placebo-NPs were present in HBsAg NPs, HBsAg loaded liposomes showed significantly lower haemolysis at some time points of 10 and 20 ng/mL equivalent concentrations ($p<0.05$). In addition, HBsAg showed significantly lower haemolysis values in comparison to HBsAg NPs and Placebo-NPs, at several time points of all three equivalent volumes.

5.8.2 Quantitative platelet aggregation

Nanoparticles were estimated for their interaction with platelets and their compatibility with coagulation system. The compatibility of nanoparticles depends on their physicochemical properties. Interaction of NPs with plasma protein is important in evaluating undesirable interactions between the coagulation system and nanoparticles, because protein binding can change physicochemical properties of nanoparticle [Mayer *et al.,* 2009; Nel *et al.,* 2009]. In case of vaccine drug delivery, it is necessary to evaluate the aggregation of platelets, because vaccine is a foreign antigen. The excessive or inappropriate aggregation of platelets upon I.M. injection of NPs may lead to thrombus formation. Therefore, evaluation of platelet aggregation in whole blood treatment is essential. Quantitative platelet aggregation was estimated using haematological counter, after incubating with Plain HBsAg, HBsAg NPs and alum

HBsAg (equivalent to 10, 20 and 30 ng/mL of HBsAg) and Placebo-NPs, (equal to volume of HBsAg NPs). PBS served as spontaneous control to assess dilution effect. Hepatitis B Antigen treated samples did not show any significant difference in platelet count than that of PBS treated samples in all concentrations, as shows in Figure 5.22. The results suggest that HBsAg is not responsible for platelet aggregation. Placebo HBsAg showed significantly lower platelet count ($p<0.05$). Lower count observed in Placebo HBsAg treated sample may be due to effect of components.

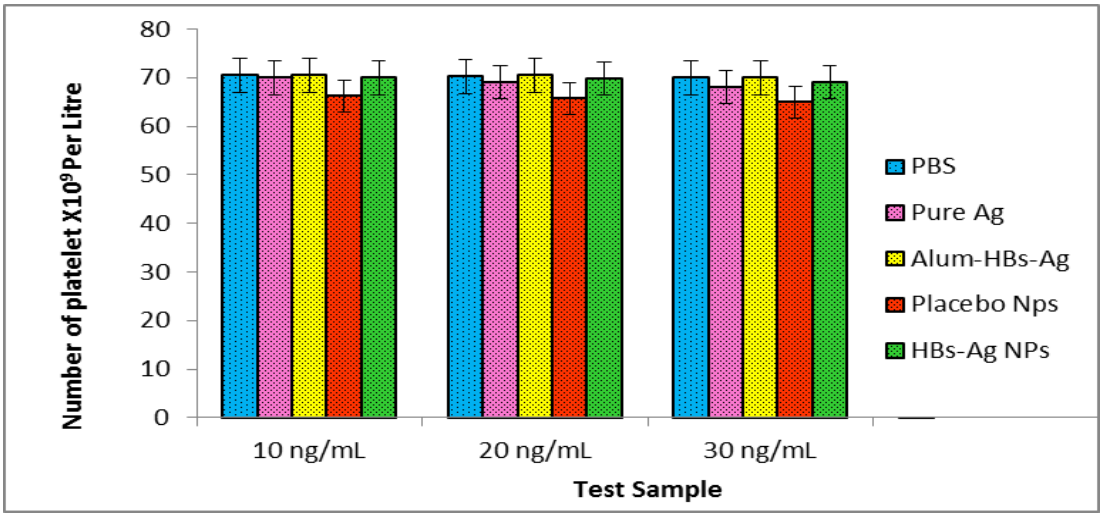

Figure 5.22: Number of platelets after addition of PBS, Pure HBsAg, Placebo-NPs, Alum HBs and HBsAg NPs at 10, 20 and 30 ng/mL

5.8.3 Qualitative platelet aggregation

The qualitative platelet aggregation in whole blood was analysed by optical microscope after incubation with plain HBsAg, HBsAg NPs, alum HBsAg (equivalent to 10, 20 and 30 ng/mL of HBsAg), Placebo-NPs (equal to volume of HBsAg NPs). Erythrocytes, white blood cells and platelets were visualized using microscope and images were taken. In Figure 5.23 the platelets are indicated by arrow marks in microphotographs. Results indicate no platelet aggregation in all three different concentrations of test

samples. Platelets were evenly distributed throughout the blood smears up on microscopic observations in all test samples. All these observations suggested that HBsAg NPs are haemocompatible and nontoxic in nature.

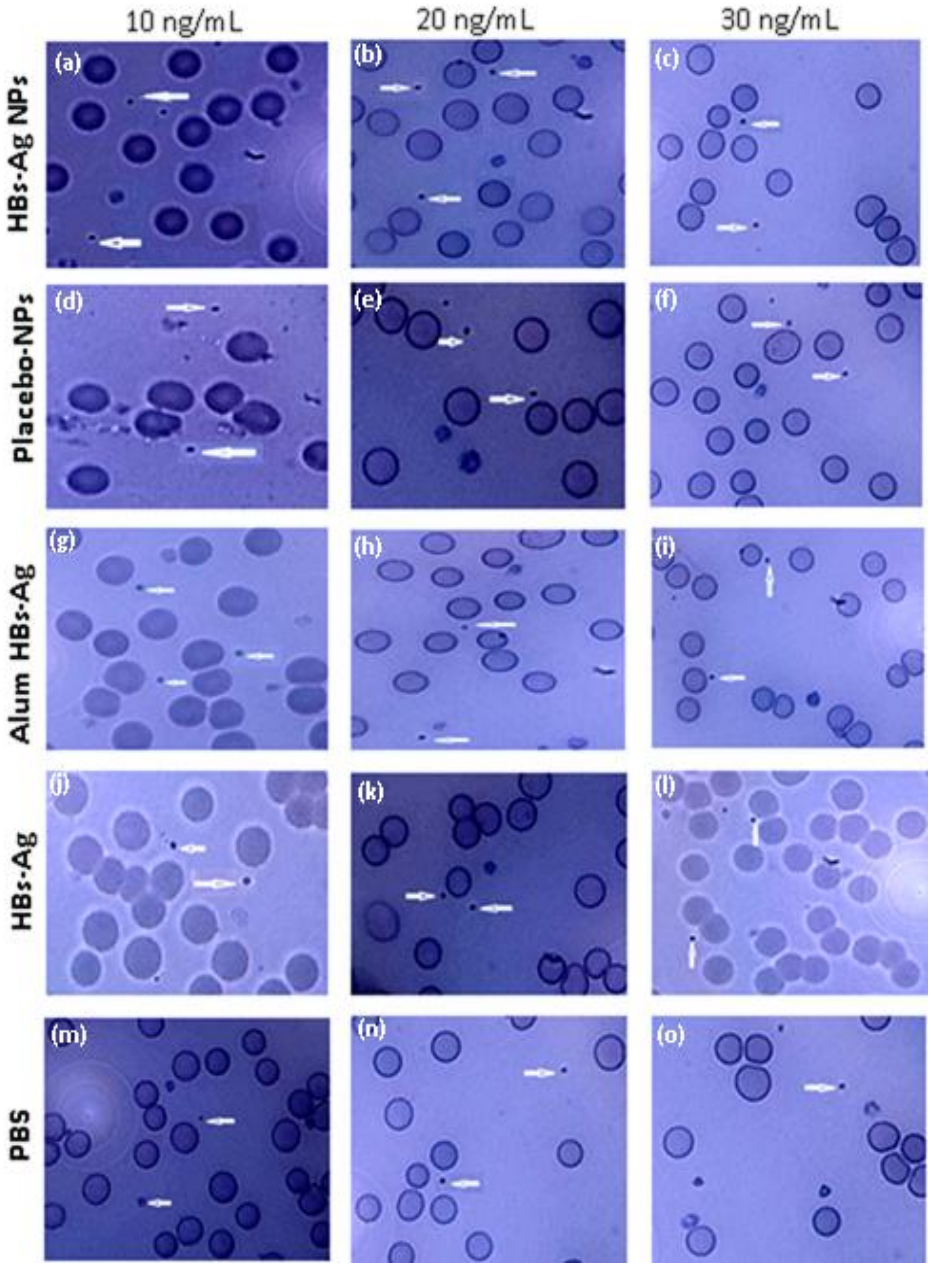

Figure 5.23: Light microscopy images of Leishman's stained whole blood samples after treating with PBS, Pure HBsAg, Placebo-NPs, Alum HBs and HBsAg NPs at 10, 20 and 30 ng/mL. Images were captured at 100×magnification

5.9 Stability study

The in-process stability of the prepared encapsulated HBsAg nanoparticles was found unaltered up to 90 days, as observed by analysis of particle size, zeta potential and encapsulation efficiency during stability studies at 30±2 ºC and 65 ± 5% RH. The optimized batch of HBsAg nanoparticles showed stability with insignificant (p>0.05) changes in particle size, zeta potential and encapsulation efficiency. The results of the stability study of HBsAg loaded NPs are presented in Table 5.8.

Table 5.8: Stability studies of HBsAg laoded nanoparticles

Days	Particles Size (nm)	Zeta Potential (mV)	Entrapment Efficiency (%)
0	266 ± 4.23	41.58 ± 0.5	92.0 ± 5.0
30	267 ± 1.28	41.02 ± 8.6	91.8 ± 3.2
60	268 ± 8.51	40.39 ± 1.6	91.1 ± 6.8
90	270 ± 2.31	40.10 ± 2.3	90.4 ± 2.9

5.10 Selection of route of administration in BALB/c mice

For the better immunological systemic and cellular antibody responses, Hepatitis B antigen loaded PLGA nanoparticles were administered via different routes viz. nasal, sub-cutaneous, oral and intra muscular injections. The antibody titre is measured by solid-phase enzyme-linked immunosorbent assay (ELISA). Different routes of administration and the antibody production responses of every route were compared and analysed statistically by one way analysis of variance (ANOVA) with Post-hoc Tukey-Kramer multiple comparisons test. The blood serum anti-HBsAg titre level obtained after intramuscular route administration of Hepatitis B antigen loaded PLGA nanoparticles was comparable with recorded titre after nasal route administered group. The highest immunoglobulin-G (IgG) level was obtained in mice administered with nanovaccine through intramuscular route, while lowest through oral route. The antibody titre of HBsAg loaded nanoparticles administered through nasal and sub-cutaneous route shows almost similar responses and no significant difference (Figure 5.24 (a)) was noticed. Whereas, significant difference in serum anti-HBsAg titre level was observed between intra muscular route and all other (oral, nasal, sub-cutaneous) routes. HBsAg loaded nanoparticles elicited a highest systemic immune response when administered through intramuscular route than nasal, sub-cutaneous and oral route.

Similarly, the immunoglobulin IgA level in blood serum was measured after 4^{th} and 8^{th} week administration of HBsAg loaded nanoparticles. The level of antibody titre is depicted in Figure 5.24 (b). After four weeks of immunization, IgA levels increases and maximum response was found in intra muscular administration while lowest response was observed in oral administration *i.e.* significant difference ($p<0.05$) was observed in comparison to other groups. The nasal and sub-cutaneous administered groups showed equal level of antibody. At end of the experiment (8 weeks), the IgA level was found to

be increased in all groups but no significant difference was observed in nasal and intra muscular administered groups.

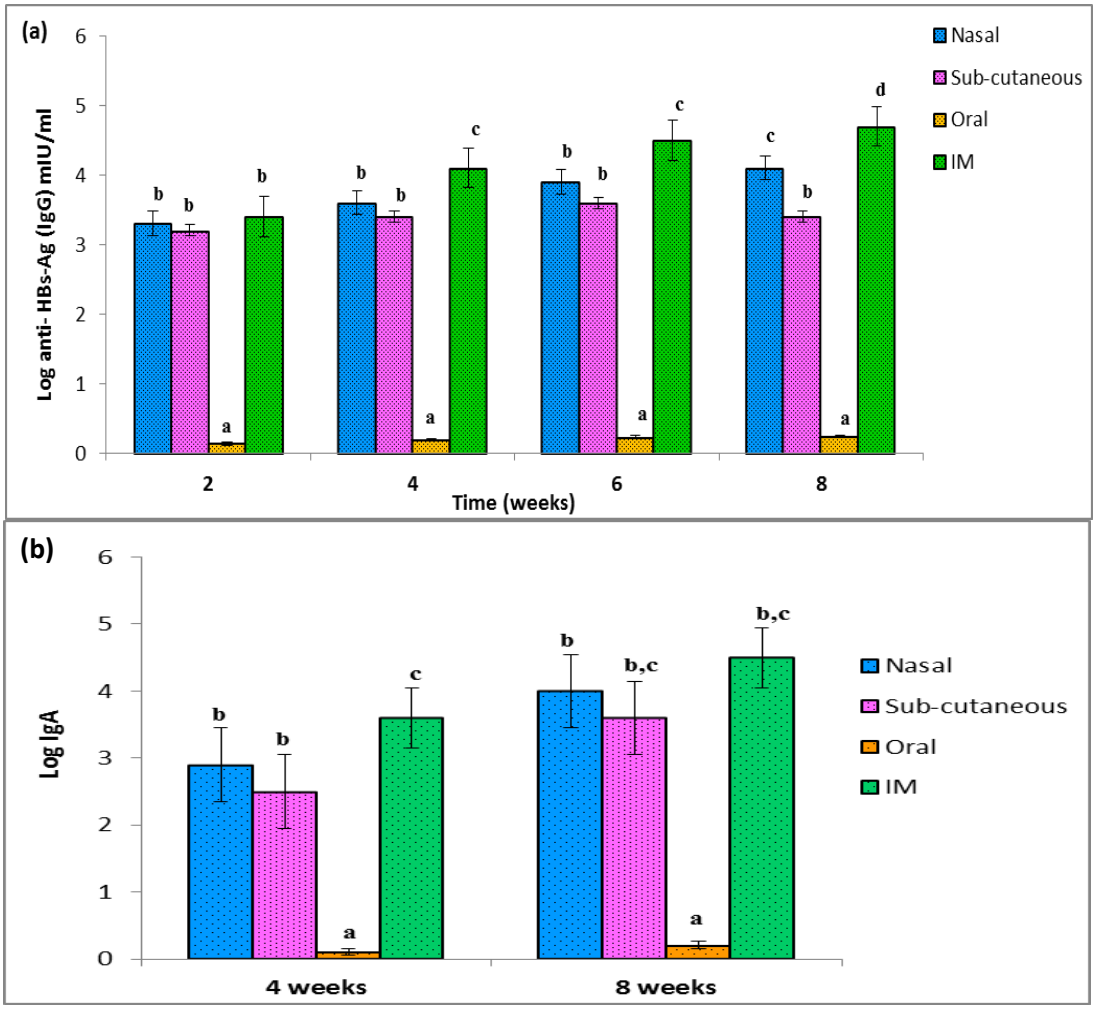

Figure 5.24: Mean ±S.D., (*n*=6) indicate effects of HBsAg loaded nanoparticles on (a) Immunoglobulin IgG levels at 2, 4, 6 and 8 weeks and (b) Immunoglobulin IgA levels at 4 and 8 weeks of immunization in BALB/c mice via different routes of administration. Different and similar alphabet bar shows significant difference and no significant difference respectively, as determine by Tukey-Kramer multiple comparisons test, significant is taken as (p<0.05)

The results indicated that nanoparticles showed greater production of IgA immunoglobulin in single dose administration. PLGA nanoparticles produced systemic immune response through I.M. route than groups receiving through nasal, sub-cutaneous and oral routes.

The other immunological endogenous cytokine markers viz. interferon-*Y* (IFN-*Y*) and interleukin-2 (IL-2) were studied at end of the experiment and the results are presented in Figure 5.25. The levels of endogenous cytokines were found to increase in intramuscularly administered BALB/c mice. Significant difference ($p<0.05$) in the level was observed in oral route, compared with all other routes of administration. The maximum level of interferon-*Y* (IFN-*Y*) was observed in intra-muscular administered groups, while equal response was observed in nasal and sub-cutaneous administered groups. Similar observation was found in interleukin-2 (IL-2) levels. Simultaneous increase in the levels of endogenous cytokine was also observed ($p<0.05$) and represented in Figure 5.25 (a) and (b).

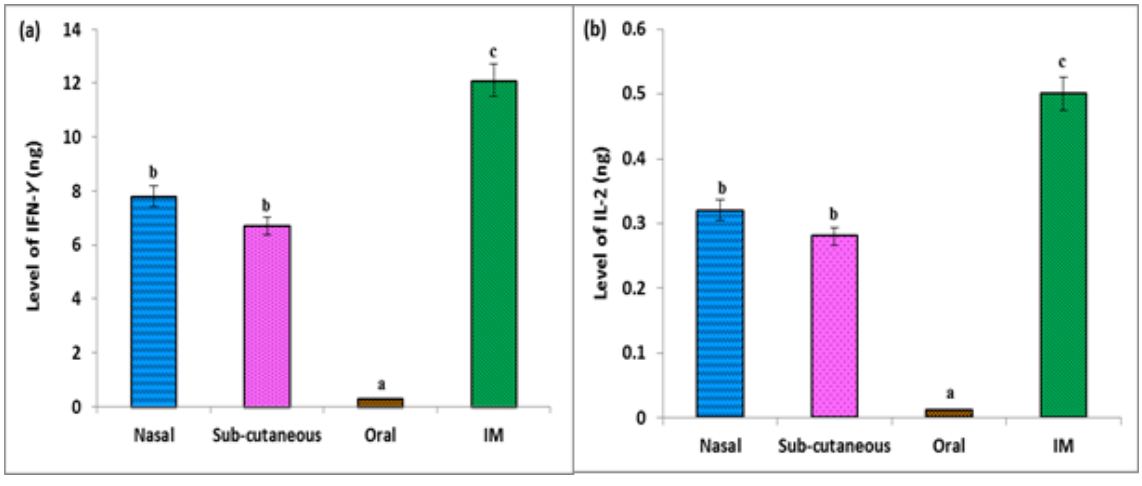

Figure 5.25: Mean ±S.D., (*n*=6) indicate effects of HBsAg loaded nanoparticles on (a) Interferon-*Y* levels at 8 weeks and (b) Interleukin-2 levels at 8 weeks of immunization in BALB/c mice via different routes of administration. Different and similar alphabet bar shows significant difference and no significant difference respectively, as determine by Tukey-Kramer multiple comparisons test, significant is taken as ($p<0.05$)

Both humoral and cellular responses were produced on administration of HBsAg loaded PLGA nanoparticles through different routes of administration viz. oral, sub-cutaneous, nasal and intra muscular. After four weeks of administration the serum antibody anti-HBsAg was found less immune effective, but after the 8 weeks of immunization it further increased. *In-vivo* evaluation of PLGA nanoparticles showed higher activity and prolonged levels of antibody in single dose of intra-muscular administration. Anti-HBsAg antibodies from the group receiving HBsAg loaded nanoparticles exhibited maximum effect, suggesting that the process of nanoencapsulation did not alter the immunogenicity of HBsAg [Nellore *et al.*, 1992].

The levels of endogenous cytokine (interferon- *Y* (IFN- *Y*) and interleukin-2 (IL-2)) in blood serum sample were estimated after 8 weeks of immunization. Both cytokines levels were found improved in mice immunized with HBsAg loaded PLGA nanoparticles. Humoral and cellular immunological response of HBsAg loaded PLGA nanoparticles administered by intra muscular route were found significantly stronger in comparison to all other routes ($p<0.05$). Moreover, HBsAg loaded PLGA nanoparticles administered by nasal route produced approximately equivalent immune response in comparison with intra-muscular route, but the nasal route was very tedious and difficulty was observed in administering the nanoparticles [Shih *et al.*, 2006].

5.11 *In-vivo* cellular internalization study

The celluar uptake behaviour of loaded nanoparticles was studied by fluorescence microscopy. The fluorescence image showed nanoparticles in deeper layers of the tissues or cells. Distribution of nanoparticles was found not uniform and fluorescence intensity dropped at depth. The sections of lymph nodes and spleen from control group showed normal histological features whereas sections of lymph nodes and spleen obtained from treated animals showed fluorescent areas indicating the uptake of HBsAg antigen (Figure 5.26 (a) and (b)). The prepared HBsAg loaded nanoparticles gets easily internalized in short period of time. After intramuscular administration of nanoparticle, it reached lymph and spleen in very higher quantity.

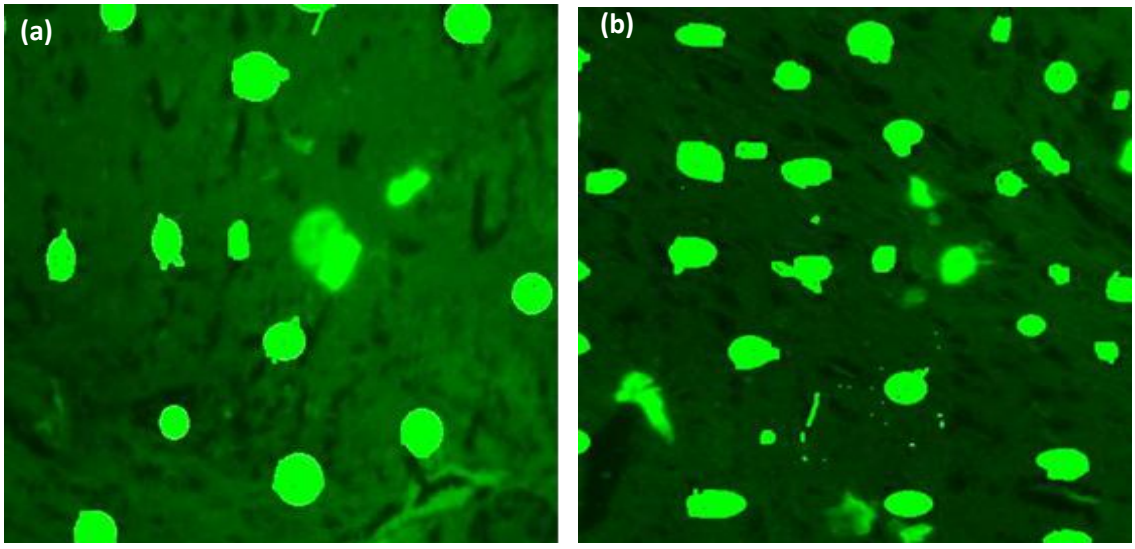

Figure 5.26: (a) Fluorescent image of lymph node after administration of FITC-HBsAg loaded NPs (b) Fluorescent image of spleen after administration of FITC-HBsAg loaded NPs

5.12 Immunological characterization and measurement of antibody levels

The humoral and cellular responses were attained after the administration of HBsAg loaded PLGA nanoparticles with or without adjuvant after single and multiple dose administration in immunogenic BALB/c mice. The measurement of antibody titre was performed by specific ELISA techniques.

HBsAg loaded PLGA nanoparticles were administered intramuscularly for induction of systemic and cellular immunological antibody responses. Normal saline, alum adsorbed HBsAg (single and booster injections), normal antigen in booster dose and HBsAg loaded PLGA nanoparticles (single and booster injections) administered groups were compared. Antibody response of each formulation at different time point was statistically analysed by one way analysis of variance (ANOVA) test. The IgG antibody titre obtained after intramuscular administration of PLGA loaded nanoparticles in single and booster dose showed similar immune response in comparison with alum-adsorbed HBsAg titre (p>0.05) Figure 5.27 (a). Insignificant difference was observed in single and multiple dose of HBsAg nanoparticles treated mice *i.e.* single dose of polymeric HBsAg nanoparticles is sufficient for antibody production.

The anti HBsAg titre of normal saline and pure antigen level showed significant difference with other groups. In Figure 5.27 (b), no significant difference was observed in the level of IgA in single and booster dose of HBsAg loaded nanoparticles and boster injection of alum adsorbed HBsAg. In single dose administered group, the IgA level was relatively low in the first month, and then it increased after two months. Equal response to booster dose of alum adsorbed HBsAg was observed.

Both the groups treated with single and booster dose of polymeric nanovaccine produced almost similar effect but the level of antibody production was higher. The *in-vivo* evaluation of PLGA nanoparticles showed higher activity (higher or prolonged antibody levels) in booster as well as single dose. In comparison to booster dose, single dose PLGA nanoparticle showed slightly lesser serum antibody levels.

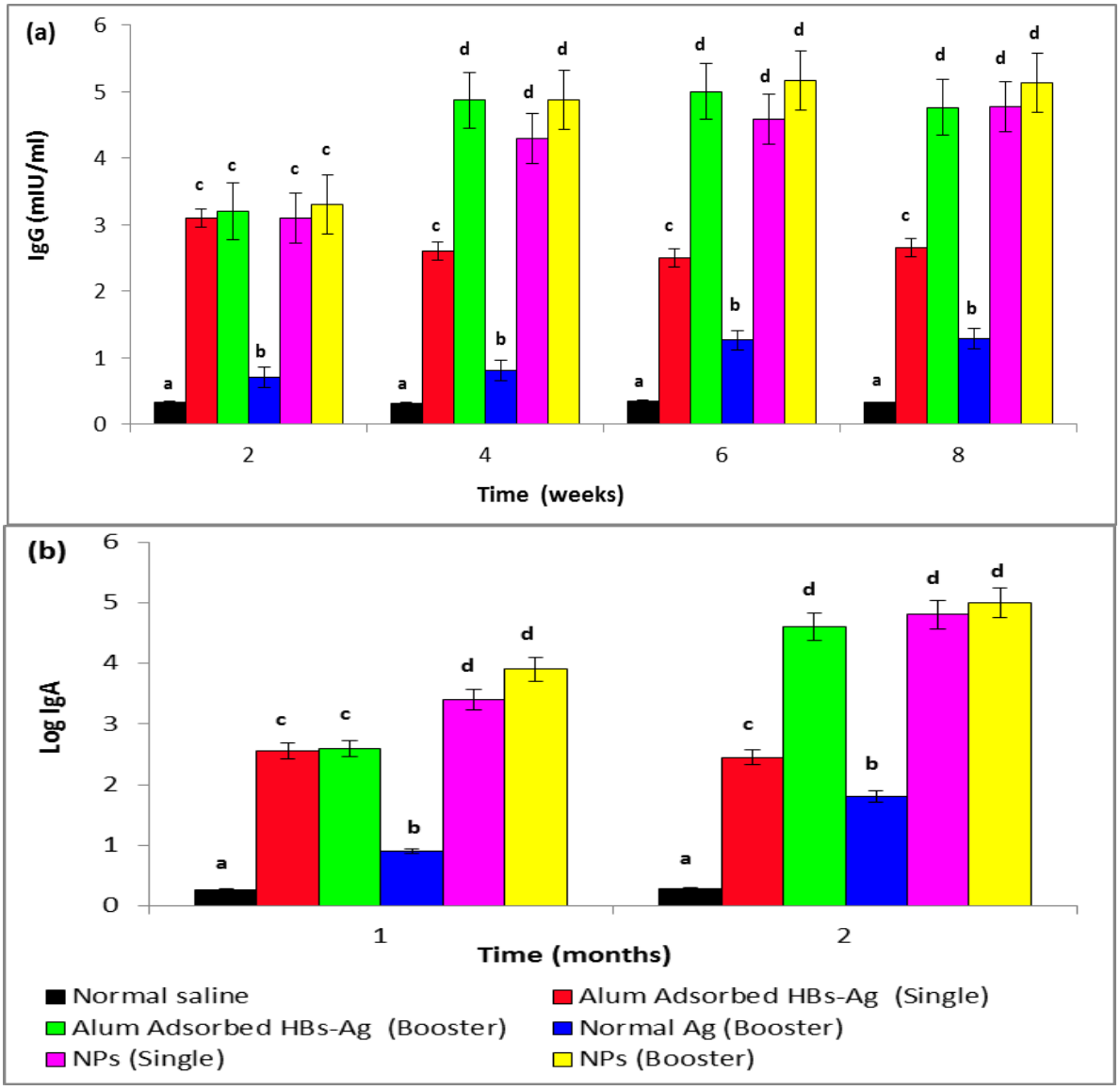

Figure 5.27: Mean ±S.D., (*n*=6) indicate the serum anti-HBsAg profile of BALB/c mice immunized with different formulations by intramuscular route on (a) Immunoglobulin IgG levels at 2, 4, 6 and 8 weeks and (b) Immunoglobulin IgA levels at 4 and 8 weeks of immunization, significant is taken as (p<0.05)

After four week of primary injection of single as well as multiple injections of HBsAg loaded PLGA nanoparticles produced anti-HBsAg response and generated an equal immune response to that of booster dose injection of alum-adsorbed HBsAg vaccine (p>0.05). *In-vivo* evaluation of PLGA nanoparticles showed higher activity in booster as well as single dose. In comparison to booster dose, single dose PLGA nanoparticles showed almost similar response.The anti-HBsAg antibodies from the groups receiving HBsAg loaded nanoparticles showed equal binding capacity to that of alum adsorbed HBsAg vaccine group. This suggests that the developed nanoencapsulation did not modify the immune activity of the HBsAg [Singh *et al.,* 1997]. Single injection of HBsAg loaded PLGA nanoparticles produced maximum responses and stayed for a longer period of time but slight different with respect to booster dose antibody production. The IgG and IgA was used as marker for the measurement of immunogenicity, where IgA is an important factor of defence against the enteropathogens and other viruses [Cleland *et al.,* 1996; Sha *et al.,* 2016]. After the administration of nanoparticles, IgG and IgA gets stimulated. Experimental results proved that a single dose of HBsAg loaded PLGA nanoparticles is sufficient for antibody production.

Single and booster dose groups of HBsAg loaded PLGA nanoparticles produced significantly equal IgA response. Immunoglobulin IgA plays a decisive role in the immune function of mucous membranes. The amount of IgA produced in association with mucosal membranes is greater than all other types of antibody [Fagarasan and Honjo, 2003]. The antibody titre (immunoglobulin IgA) obtained after intramuscular administration of PLGA loaded nanoparticles at single and booster dose was comparable with titer recorded after administration of alum- adsorbed HBsAg. Normal antigen administered booster dose and normal saline administered mice groups

produced no desire effect. Group receiving alum adsorbed HBsAg, produced no sufficient serum antibody in single dose while booster dose produced adequate IgA. But in case of single and booster dose nanovaccine administered groups almost similar and higher production of antibody levels of IgA were observed. The *in-vivo* evaluation of PLGA nanoparticles showed higher action and prolonged antibody production in booster as well as single dose administration. In comparison to booster dose, single dose of PLGA nanoparticle showed slightly lesser serum antibody levels. The IgA response of HBsAg loaded PLGA nanoparticles in booster dose was seemed to be significant in comparison with HBsAg loaded PLGA nanoparticles in single dose ($p < 0.05$).

- **Measurement of cytokines levels**

Cytokines are having the quality to bind specific receptors on target cells with high affinity to the cells that respond to cytokines. The immune activity measure, in case of HBsAg loaded NPs involves mainly two markers viz. Interleukin 2 (IL-2) and Interferon gamma (IFN-Y). The comparative response of endogenous cytokine levels (IL-2 and IFN- *Y*) in blood serum, after the administration of HBsAg loaded PLGA NPs and alum adsorbed vaccine are shown in Figure 5.28 (a) and (b).

Endogenous cytokine levels (interferon- *Y* (IFN- *Y*) and interleukin-2 (IL-2)) were estimated in blood serum after 8 weeks of booster immunization with different formulations. The levels of both cytokines were measured in mice immunized with HBsAg loaded PLGA nanaoparticles and compared to those immunization recorded for control group (Figure 5.28 (a) and (b)). Humoral and cellular immunological response of HBsAg loaded PLGA nanoparticles were found to be significantly stronger in comparison with control group ($p < 0.05$). This antigen loaded PLGA nanoparticles

based novel delivery system can be preferred over traditional vaccines for improved patient compliance.

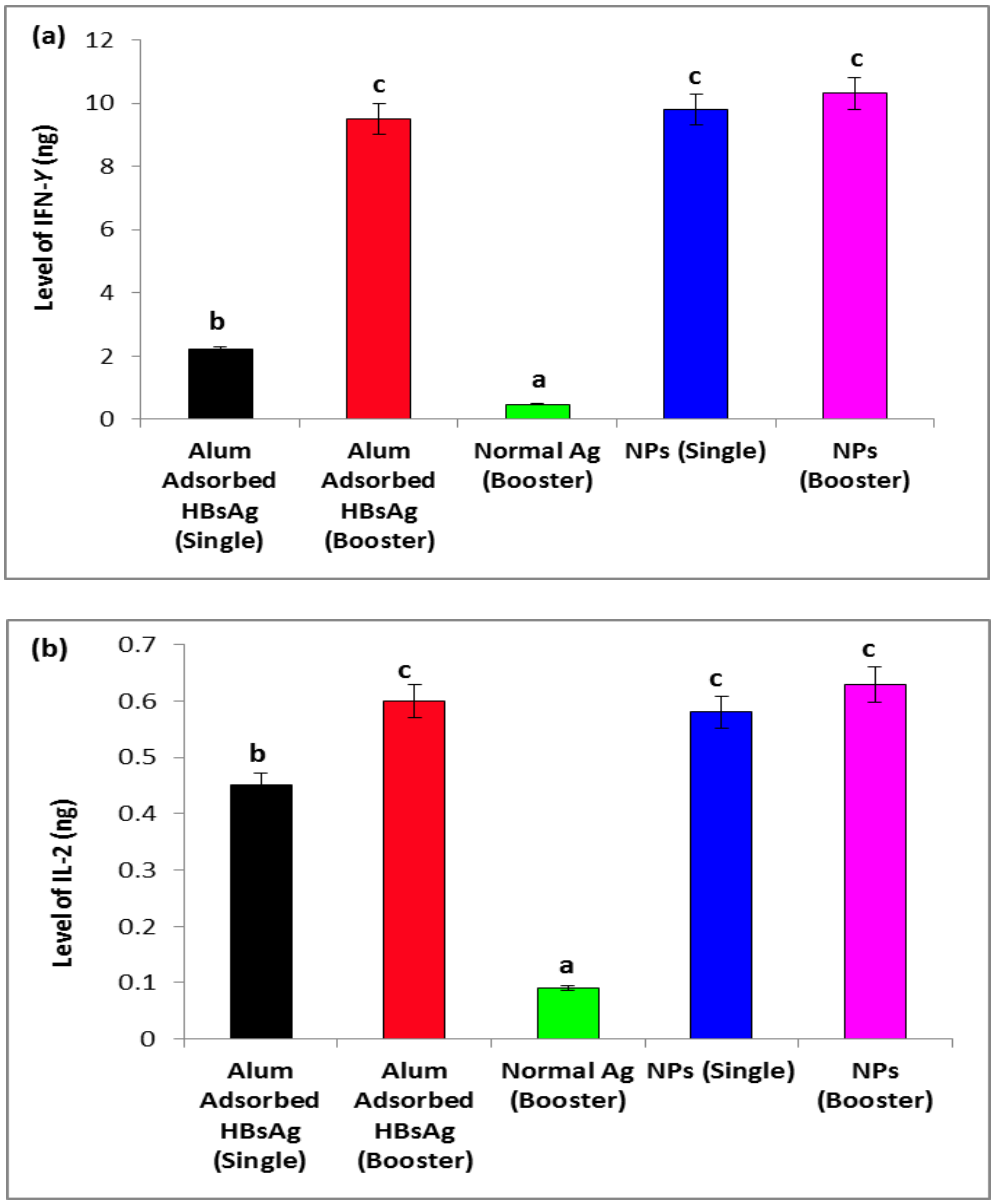

Figure 5.28: Mean ±S.D., (*n*=6) indicate the serum anti-HBsAg profile of BALB/c mice immunized with different formulations by intramuscular route on (a) Interferon-*Y* levels at 8 weeks and (b) Interleukin-2 levels at 8 weeks of immunization, significant is taken as ($p<0.05$)

5.13 *In-vivo* Lymphocyte and T cells proliferation study

5.13.1 Lymphocyte proliferation test in BALB/c mice

Lymphocyte stimulation and proliferation by specific antigen or through Hepatitis B antigen loaded nanoparticles results in synthesis of RNA, some amount of protein, DNA and production of lymphokines; it is followed by proliferation and differentiation of various effector and memory cells. The ability of different samples to stimulate the proliferation of human T-cell was assessed by the BrdU incorporation method. A significantly high cellular proliferative response (as indicated by stimulation index; SI) was observed in mice immunized with HBsAg loaded PLGA nanoparticles formulations as compared to blank nanoparticles and plain HBsAg. SI was found to be more for PLGA (50:50) HBsAg-NPs than others (Figure 5.29, Table 5.9). The experimental results suggest that HBsAg loaded NPs vaccines are more safe and effective means for measurement of T-cell immune response in healthy and immune supressed individuals.

Table 5.9: Stimulation Index of different samples like Blank NPs, Plain HBsAg and HBsAg loaded NPs

S. No	Sample Name	Stimulation Index (SI) ConA= 10µg/ml	Stimulation Index (SI) HBs-Ag= 5µg/ml
1.	Blank NPs	3.5	1.5
2.	Plain HBsAg	10	3.0
3.	Alum-HBsAg	15	4.5
4.	HBsAg NPs	24	5.5

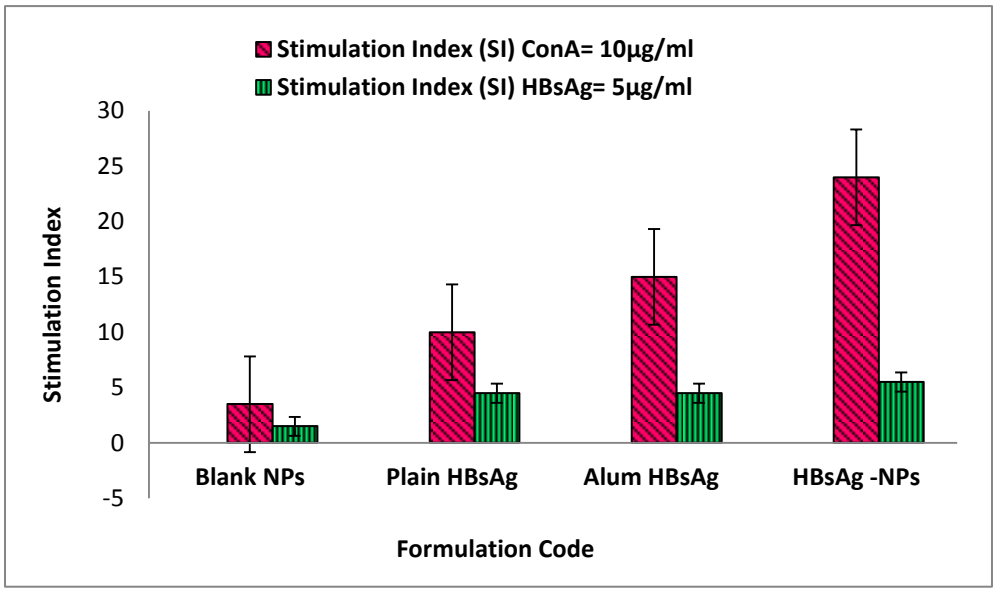

Figure 5.29: Graphical representation of lymphocyte proliferative Stimulation Index of blank NPs, plain HBsAg, alum HBsAg and HBsAg-NPs

5.13.2 T cell proliferative study in human peripheral blood

When the native T cells respond to a foreign antigen, they proliferate and differentiate in short period. T cell proliferative response assay was performed and found cells with rapid proliferation rate. The ability of different samples to stimulate human T-cell proliferation was assessed by BrdU incorporation method [Tough and Sprent, 1994].

Maximum proliferation index was observed in case of HBsAg loaded NPs (46.3%). The high levels of T-cell responses were observed due to a Viral Superantigen Effect (Figure 5.30). The viral superantigenic effect means defence mechanism against the immune system in some individuals. The superantigens are viral agents that have a strong effect on the immune response of the host cells. Their main and initial target is T lymphocyte, as well as whole cascade of immunological reactions. It is also proved that, the

interferon- I (IFN-I) plays an important role for the proliferation of the T cells. During the viral infection, large amount of interferon is secreted [Sprent *et al.,* 2000]. Some of the cytokines are responsible for the growth of the T cells. Cytokines, such as IL2, stimulate T cells proliferation rate and they proliferate in concentration dependent manner. The level of T cells proliferation can be used as the measurement of IL2 concentration. The increasing level of IL2 indicates stimulation of immunoglobulin. T cells proliferation shows defence against the attack of foreign substance and the prepared HBsAg loaded nanoparticles arrest the proliferation of T cells without damaging the cells.

Table 5.10: Proliferation Index of different samples

S. No.	Sample Code	% Proliferation Index
1.	Blank NPs	21.6
2.	Plain HBsAg	29.8
3.	Alum HBsAg	43.2
4.	HBsAg- NPs	46.3

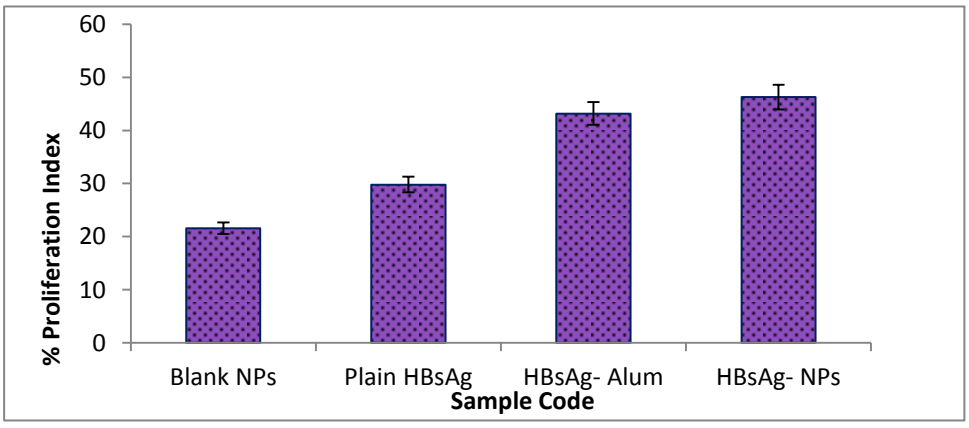

Figure 5.30: Graphical representation of T cell proliferative assay of blank NPs, plain HBsAg, HBsAg NPs

5.14 Assessment of immunological parameter in Humanized Xenograft model

An *in-vivo* humanized model or human/mouse chimeric mode is an extremely valuable tool for the study of new vaccine strategies for the generation and detection of antigen specific immunoglobulin G (IgG) secreting B cells and interferon-*Y* secreting T cells. Therefore, the occurrence of human immunoglobulin and specific antibodies in chimeric mouse sera indicated the presence of functional B and T cells in the mice model, direct detection of such cells which was impossible [Bocher *et al.,* 1999]. Chimeric mice/xenograft mice transplanted with human PBMC from HBV-immunized donors spontaneously developed significant levels of serum anti-HBs antibodies. They were further vaccinated with HBsAg loaded polymeric NPs *in-vivo*. As a result of vaccination developed mice showed high serum antibody response levels. It is associated with an increase of anti-HBs–secreting B cell frequencies and T cells secreting HBs-specific IFN-*Y* activity. The cytokine secreted by Hepatitis B virus antigen specific T cells was confirmed by *in-vitro* studies. It was reported that IFN-*Y* and IL-2 were secreted by Hepatitis B virus antigen specific T cells, derived from naturally developed HBV-immunized individuals or HBs vaccine recipients [Sylvan and Hellstrom, 1990; Tsutsui *et al.,* 1991; Bocher *et al.,* 1999].

The detection of antigen-specific B-cell and T-cell responses in humanized chimera mice has been difficult due to the lack of sensitive B-cell and T-cell assays. Also, when the chimera mice were transplanted with PBMCs of chronic HBV carriers, they did not show anti-HBs antibodies in serum. This defective problem of anti-HBs production was not protected by vaccination with a conventional recombinant HBs vaccine (marketed vaccine).

Characterization of functional human B and T cells at different time points in the human/mouse radiation chimera mice

Peripheral Blood Mononuclear Cells (PBMCs) were obtained from more than six month of HBV infected/ immunized human donors. HBV infection has serologically positive for HBsAg, HBcAg and anti-HBe antibodies (Table 4.6). Anti-HBs–secreting B cells and HBs specific IFN-*Y* secreting T cells were found in the PBMC of donor blood in high frequencies. The Aspartate Aminotransferase and Alanine Aminotransferase were also measured in donor's blood. The ratio of AST (Aspartate Aminotransferase) and ALT (Alanine Aminotransferase) was found to be less than one; it indicates non-alcoholic fatty liver disease and viral hepatitis.

When a chimeric BALB/c mice, (transplanted with 8 to 10X 10^7 infected PBMC), were vaccinated either with prepared polymeric HBsAg nanoparticles, with or without tetanus vaccine or normal saline. The mice were divided into three groups, each group having six animals. The first group of mice given by the same protocol condition was vaccinated with antigens vaccine but did not receive TT. The second group of mice received only tetanus toxoid vaccine. A third group of mice given by the same protocol condition was vaccinated with both antigens vaccine as well as receive TT. The vaccinated mice shows strongest specific immune response is observed in the human/mouse radiation chimera mice during the around two weeks of post-transplantation. The blood serum and cells were collected approximately in 1, 6, 12 and 18 days after PBMC transplantation and vaccination. The estimation of B cells secreting immunoglobulins IgG and T cellsspecific IFN-Y was measured in ELISA technique.

- **Examination of IgG-secreting B cells**

The human/mouse radiation chimera mice exhibit high levels of IgG, acquired on some days of post-transplant. The amounts of such B cells were studied in the serum of chimeric mice. The challenge is recovery of the mice cells after being transplanted with PBMCs of HBV donors. HBsAg vaccine mice exhibited substantially greater frequencies of anti-HBs as compared with unvaccinated control mice (Figure 5.31). It was found that immunoglobulin in PBMCs transplanted chimera mice of chronic HBV carriers was highest on starting day of post transplantation. The excess production of the immunoglobulin in chimera mice was also observed. Levels are again measured on last days of experiment. The immunoglobulin level in approximate maintained in group treated with vaccine. The group receive only saline/TT not significant change observed *i.e*, the level of immunoglobulin was higher.

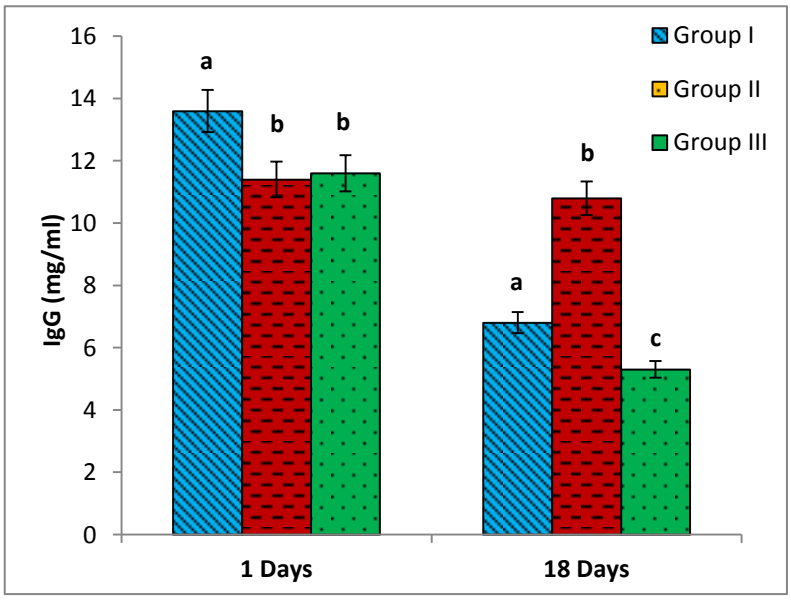

Figure 5.31: Levels of human immunoglobulins (IgG) in sera of chimeric mice transplanted with PBMCs of HBV-immunized carriers. BALB/c chimeric mice were transplanted with PBMCs and vaccinated with HBsAg loaded polymeric particles or TT. Sera were collected at days first and after 18 days

The first group which receive only vaccine but not taken tetanus toxoid, the level of IgG was decreased but in comparison to vaccine group (Group III) less amounts was observed. The results indicate that TT vaccine was also helps in increasing the activity of the polymeric nanoparticles vaccine.

- **Examination of secreting T cells**

Antigen-specific T-cell is need of B cells which helps for proliferation, differentiation and effective production of specific type of antibodies. Determination of the total number of functional T cells, measure the frequencies of T cells secreting response interferon *Y* (IFN- *Y*). All PBMCs transplanted mice found HBs-specific less amount of IFN-*Y* secreting activity on starting days. After vaccination on 18th days, the frequency of IFN-*Y* secreting cells reached its normal level in both group I and III (Figure 5.32).

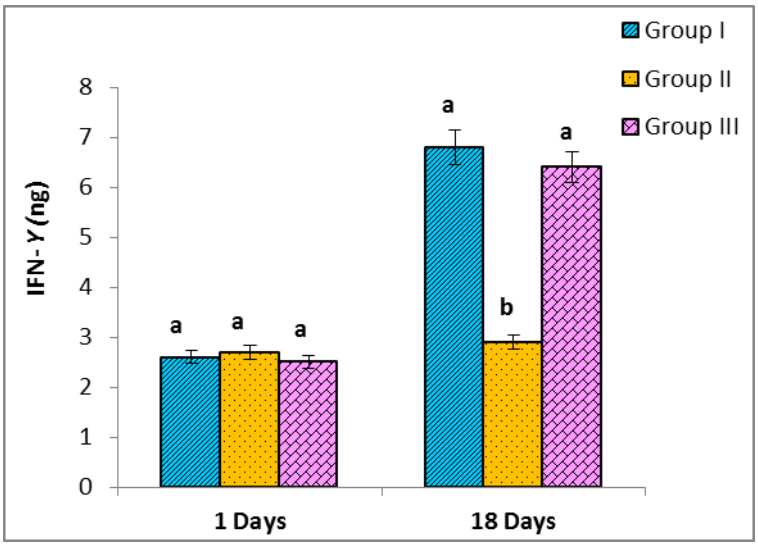

Figure 5.32: Cytokine (IFN-*Y*) in sera of chimeric mice transplanted with PBMCs of HBV-immunized carriers. BALB/c chimeric mice were transplanted with PBMCs and vaccinated with HBsAg loaded polymeric particles or TT. Sera were collected at days first and after 18 days

The group II showed hyper immune response (more interferon levels), which receive tetanus toxoids and normal saline. TT vaccination of control and test mice of the same donors were examined for TT-specific T cells response. It also observed that after vaccination with TT not only higher serum levels of anti-TT antibodies, also high frequencies of TT specific IFN-*Y* was found in mice transplanted with PBMCs**.**

- **Detection of HBsAg and anti-HBsAb by ELISA assay method**

In chimera mice, having infected PBMC viral replication in the liver is common but due to presence of vaccination, not in sufficient/properly. Presented viral DNA in chimera mice was purified from blood, and viral genomes were measured by a quantitative PCR assay technique. Group II & III mice developed high-titer anti-HBs antibody (HBsAb), than group I. However the amount of viral HBsAg was reduced. Large amount of viremia was detected on first day of experiment. Viremia subsequently declined through day 6^{th} and viral titers was decreases more in 18^{th} day. The amount of HBV surface antigen (HBsAg) was higher on initial day, after that, serum HBsAg decline slowly and the concentration was reached lowest on day 18^{th}. The antibodies specific for HBsAg became detectable in the blood serum. The highest level of HBsAg antibody was found in group III.

On initial day HBsAg antibodies level were lowest (35.6±3.5 mIU) and highest levels were on day 18^{th} (35621±4.6 mIU). The group II, which received only saline did not shows significant increment of antibodies production. The group I had low antibody comparison to group III (Figure 5.33 (b)). The results indicated that TT is having quality to increase the activity of the Hepatitis B polymeric vaccine activity.

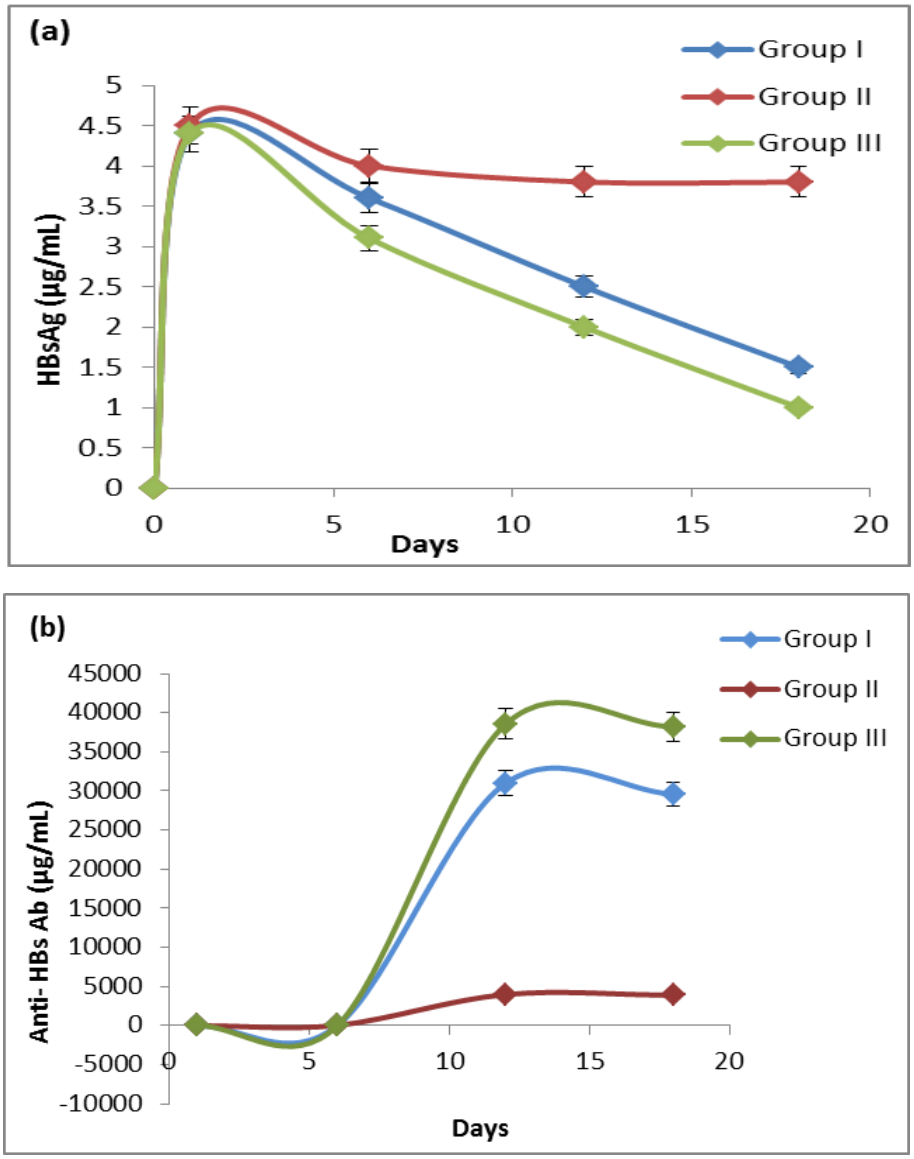

Figure 5.33: (a) HBsAg and (b) Anti-HBs antibody levels in serum of chimeric mice transplanted with PBMCs of HBV-immunized carriers. BALB/c chimeric mice were transplanted with PBMCs and vaccinated the same day with HBsAg loaded polymeric particles. Sera were collected at the indicated time points and assessed

- **Detection of HBcAg**

The Hepatitis B viral core protein (HBcAg) expression was examined by immune histochemical staining liver cells on day 1st and 18th. Core proteins are mostly randomly distributed throughout the liver lobule. HBcAg expression highest on first day and the frequency of HBcAg-positive hepatocytes decreased on day 18th. HBcAg-positive hepatocytes were surrounded by inflammatory cells, therefore decreasing of hepatocytes increasing the inflammatory cells. Figure 5.34 (A) and (B) are shows the vaccinated group chimera mice liver cells, which received the polymeric nanoparticles vaccine as well as TT.

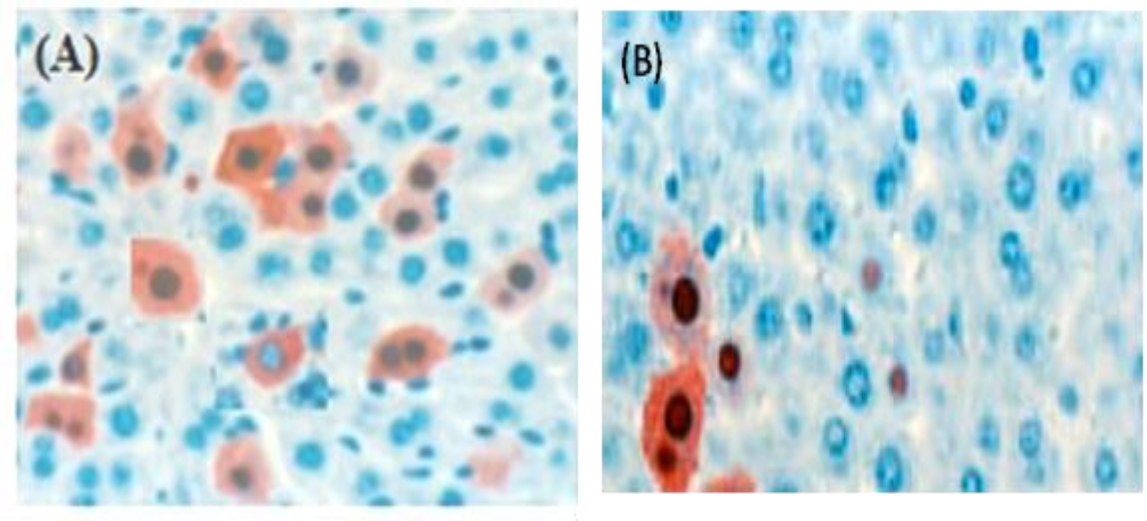

Figure 5.34: HBcAg expression in the liver on (A) day 1 and (B) days 18

- **Quantitation of Viremia by Real-time PCR**

When a HBV infected PBMC was transferred in human/mouse radiation chimeras mice, large amounts of Hepatitis B viral replicated in these mice and viremia as well as viral like antigens particles was observed in blood. It was also supress/ negative responses the chimera mice immune response after vaccination. The blood serums of all chimera mice were tested for the presence of HBsAg and HBcAg. HBV-DNA could be detected

and assessed by PCR in given time period. All mice groups shows the average concentration of HBV surface antigen is highest ($3.8X10^6$ ±2 copies/mL) at the first day of the infection. After day by day the amount of viremia was slowly decreases continuously in blood. The group which received polymeric vaccine as well as TT were $1.9X10^6$ ±2.8 copies/mL and $0.8X10^6$ ±8.9 copies/mL was found in days six and twelve (figure 6) and last day of experiments minimum amount of viremia was observed ($0.25X10^6$ ±3.6 copies/mL) present in Figure 5.35. The chimera mice group which received only vaccine showed comparatively high level of viremia in blood ($0.35X10^6$ ±3.5 copies/mL) in eighteen day of experiments. The second group of mice found only saline/TT showed high levels of HBV in blood, and amount of virus was increases day by day [Segall *et al.*, 1996]. Results indicated that, the vaccinated group of mice having ability to production of antibodies as well as control the growth of viremia in chimera mice transplanted with PBMCs.

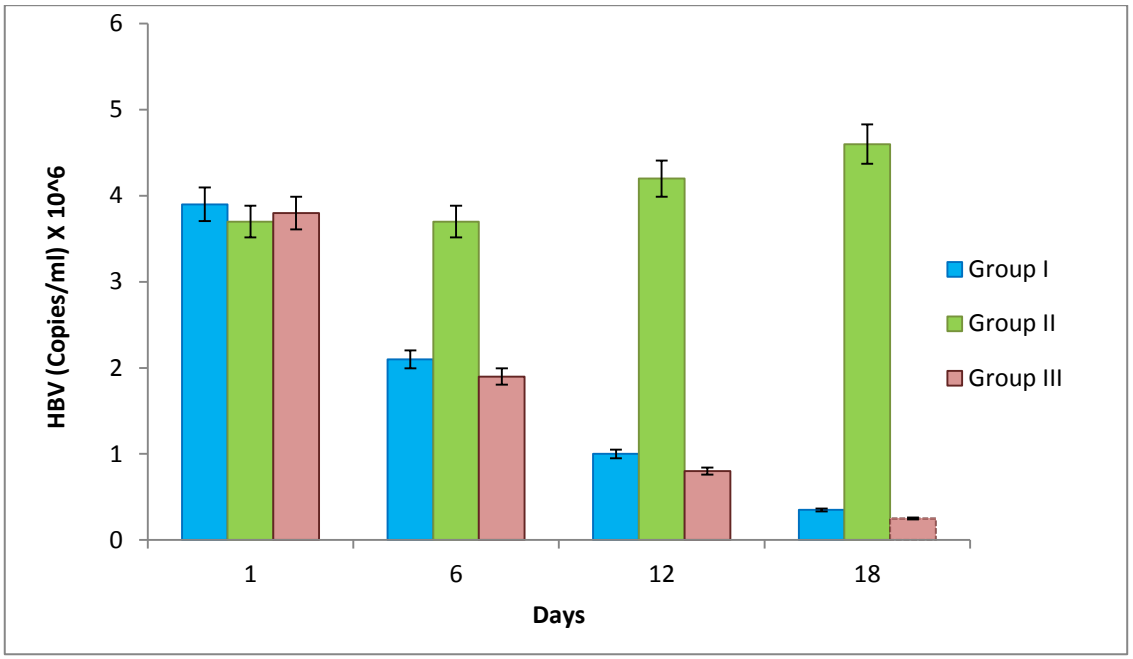

Figure 5.35: Viremia concentration of sera of chimeric mice transplanted with PBMCs of HBV-immunized carriers. BALB/c chimeric mice were transplanted with PBMCs and vaccinated with HBsAg loaded polymeric particles or TT. Sera were collected at days first, 6, 12 and 18

The high HBV viraemia load suggesting that suppress of HBV specific Th cell responses, because this core antigen–specific T cell was reversible. In this, all phenomena an early innate immune response, NK cells mediates and IFN-Y dependent down regulation of viral replication. The successive virus-specific T-cell response led to the eventual clearance of HBV by cytolytic and noncytolytic mechanisms. The developed mouse immune system is capable of both modes of immune control system because they have both been induced in the transgenic mouse model [Kakimi *et al.*, 2000; Guidotti *et al.*, 1996]. The developed mice model show virus-specific CTL (Cytotoxic T Lymphocytes) response. The relationship between the HBV-specific CTL response and viral clearance remains to be determined, as do the presence and functional impact of any innate immune response. Generally, this manipulated xenograft mice are easy to analyse in comparison to chimpanzee. The specific cytotoxic T lymphocytes response IFN-Y and any innate immune response are important for presence in mice model. The cytotoxic T lymphocytes response is capable to remove virus and viral-like particles.

- **Viral Gene Expression in chimera mice**

The role of cellular and humoral immune response on the Hepatitis B virus expression was checked by hydrodynamic transfer of human infected PBMCs cell in immunodeficient mice, which having lack functional B and T cells, as well as natural killer (NK) cell activity [Eren *et al.*, 1998]. After the transfer of PBMCs cells in mice, viral DNA replications and its intermediates were detected in the liver and blood of mice in 6 days. The B cells were also studied in the serum of chimeric mice. HBs vaccinated group of mice exhibited substantially greater frequencies of anti-HBs as compared with unvaccinated control group mice. It was found that highest numbers of immunoglobulin in PBMC transplanted chimera mice of chronic HBV carriers on

starting day of post transplantation. All PBMCs transplanted mice were found to be HBs-specific more IFN-*Y* secreting activity on starting days. After the vaccination, the frequency of IFN-*Y* secreting cells was reach on normal state receiving polymeric vaccine. In starting large amounts of HB viral replicated in these mice and supress after vaccination. The blood serums of all chimera mice were tested for the presence of HBsAg and HBcAg. HBV-DNA could be detected and assessed. The expression of the HBcAg was examined by immunohistochemical staining of liver (Figure 5.36). The disappearances of the HBcAg-positive hepatocytes from the liver of treated mice and development of HBV-specific T cell response. The persistence of viral gene expression in irradiated and bone marrow transplanted BALB/c mice which received infected PBMCs for extended periods of time. In the absence of immune responses, vaccine helps for production of specific immune immunoglobulin and interferon. An immune response strongly suggests that it play a central role in the elimination of HBV-positive hepatocytes in the immune competent mice.
